

Design, Synthesis, and Structure–Activity Relationships of 1-,3-,8-, and 9-Substituted-9-deazaxanthines at the Human A_{2B} Adenosine Receptor

Angelo Carotti,^{*,†} Maria Isabel Cadavid,[§] Nuria B. Centeno,^{||} Cristina Esteve,[⊥] Maria Isabel Loza,[§] Ana Martinez,[‡] Rosa Nieto,[‡] Enrique Raviña,[‡] Ferran Sanz,^{||} Victor Segarra,[⊥] Eddy Sotelo,[‡] Angela Stefanachi,[†] and Bernat Vidal[⊥]

Dipartimento Farmaco-chimico, Università di Bari, via Orabona 4, I-70125 Bari, Italy, Departamento de Química Organica and Departamento de Farmacología, Universidad de Santiago de Compostela, E-15782 Santiago de Compostela, Spain, Unitat de Recerca en Informàtica Biomèdica (GRIB), IMIM-UPF, C/ Dr. Aiguader 80, E-08003 Barcelona, Spain, and Almirall Prodesfarma S.A., General Mitre, 151 E-08022 Barcelona, Spain.

Received June 30, 2005

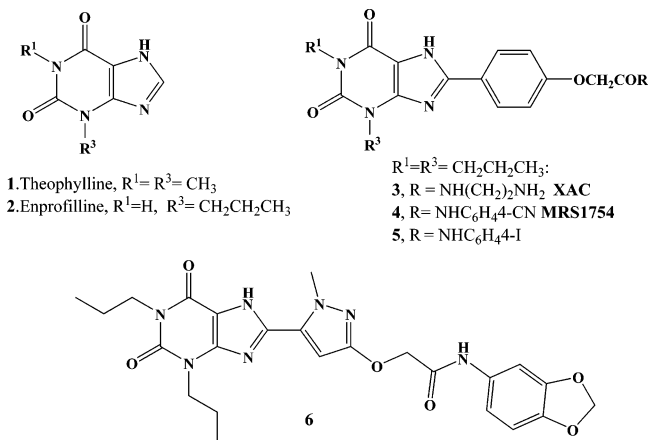
Over two hundred 1-, 3-, 8-, and 9-substituted-9-deazaxanthines were prepared and evaluated for their binding affinity at the recombinant human adenosine receptors, in particular at the hA_{2B} and hA_{2A} subtypes. Several ligands endowed with sub-micromolar to low nanomolar binding affinity at hA_{2B} receptors, good selectivity over hA_{2A} and hA₃, but a relatively poor selectivity over hA₁ were obtained. Good antagonistic potencies and efficacies, with pA₂ values close to the corresponding pK_is, were observed in functional assays in vitro performed on a selected series of compounds. 1,3-Dimethyl-8-phenoxy-(*N*-*p*-halogenophenyl)-acetamido-9-deazaxanthine derivatives appeared as the most interesting leads, some of them showing outstanding hA_{2B} affinities, high selectivity over hA_{2A} and hA₃, but low selectivity over hA₁. Structure–affinity relationships suggested that the binding potency at the hA_{2B} receptor was mainly modulated by the steric (lipophilic) properties of the substituents at positions 1 and 3 and by the electronic and lipophilic characteristics of the substituents at position 8. A comparison among affinity and selectivity profiles of 9-deazaxanthines with the corresponding xanthines suggested some possible differences in their binding mode.

Introduction

Bronchial asthma is a severe, widespread disease with inherent variability and unpredictable exacerbations ranging from mild to fatal.¹ Despite the recent considerable advancements in the understanding of the etiopathogenesis of the disease,² the ultimate mechanisms underlying its onset and development remain elusive, and this precludes a rational approach for the discovery of new and more efficient therapeutic agents. Indeed, the therapy of asthma remained substantially unchanged in the past decades, with the inhaled β₂-adrenoceptor agonists and corticosteroids still constituting the main drugs for its first line treatment.³ As a second line treatment, leukotriene receptor antagonists⁴ and the monoclonal antibody IgE immunomodulator omalizumab⁵ are occasionally used. However, in many patients, the treatment of asthma is not optimal, and this may impact both morbidity and mortality. There is therefore an urgent need for alternative, more resolute, and safer drugs to efficiently cope with this life-threatening and disabling disease.

Recently a role of adenosine in asthma, longly advocated,⁶ has been proved on the basis of key experimental evidence such as the increase of adenosine concentration in hypoxia and cellular inflammation in bronchoalveolar fluids of asthmatics and in plasma (upon a contact with allergenes).⁷ Moreover, adenosine (in the form of AMP) induces bronchoconstriction in asthmatics but not in healthy individuals.⁸ Finally, theophylline, a dimethylxanthine with a well established role in the

Chart 1. Xanthine Derivatives with Antiasthmatic (**1** and **2**) and Selective A_{2B} AdoR Antagonistic Activities (**3–6**)



therapy of asthma, proved to block selectively the AMP-induced bronchoconstriction.⁷ The bronchodilating activity of theophylline **1** and its structural analogue enprofylline **2** (Chart 1) has been recently attributed to a selective, albeit small, antagonism at the A_{2B} adenosine receptor (AdoR),⁷ one of the four distinct AdoR subtypes (e.g. A₁, A_{2A}, A_{2B}, A₃) on which adenosine acts.^{9,10} These findings prompted several groups to design and test a huge number of xanthine derivatives in the search for new, more potent, and A_{2B}-selective ligands.^{11–17} Weakly selective A_{2B} antagonists have been initially discovered,⁸ and only in the past few years have more potent and A_{2B}-selective 1,3,8-trisubstituted xanthines, such as XAC, MRS1754, and 1,8-disubstituted xanthines such as **6** (Chart 1), been found.^{13,18–27}

While xanthine derivatives constitute, along with purine nucleoside analogues and condensed tricyclic nitrogen heterocyclic derivatives,^{28–32} one of the most exploited class of AdoR ligands, 9-deazaxanthines [9-dAXs, (1,3-dialkyl-6(7)-(di)sub-

* Corresponding author. Tel.: ++39-080-5442782; fax: ++39-080-5442230; e-mail: carotti@farmchim.uniba.it.

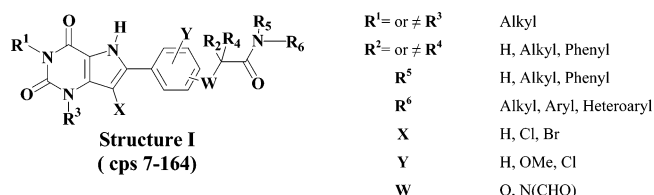
[†] Dipartimento Farmaco-chimico, Università di Bari.

[‡] Departamento de Química Organica, Universidad de Santiago de Compostela.

[§] Departamento de Farmacología, Universidad de Santiago de Compostela.

^{||} Unitat de Recerca en Informàtica Biomèdica (GRIB)-

[⊥] Almirall Prodesfarma S.A.

Chart 2. General Structure and Main Structural Variations of Designed 9-dAX AdoR Ligands

stituted-1*H*-pyrrolo[3,2-*d*]pyrimidine-2,4(3*H*,5*H*)-diones]) have been only rarely studied, especially for their antagonistic activity at the A_{2B} receptor.³³ For this reason, some years ago we began a systematic, long-term study first addressing an easy, efficient, and fast synthetic pathway to fully functionalized 9-dAXs and then a deep investigation of their biological and pharmacological properties. Our goal was to discover potent ($K_i < 30$ nM) antagonists of the human A_{2B} receptor (*hA*_{2B}) with at least >100-fold selectivity over *hA*_{2A} and, possibly, over the other two AdoR subtypes, namely *hA*₁ and *hA*₃. Preliminary accounts of this research have been published.^{34,35}

Suitable substituents were introduced in several positions of the 9-dAX nucleus to properly explore the structure–affinity (SAR) and structure–selectivity relationships (SSR). The main structural variations on the 9-dAX nucleus were initially made at the positions 1 and 3 (with alkyl or functionalized alkyl substituents), at position 7 (with a simple *N*-methylation),³⁵ and at position 8 where mainly para-substituted phenyl groups were introduced. Then, following the interesting results obtained by Jacobson et al. on xanthines,⁸ in the para-position of the 8-phenyl ring was placed an oxyacetamido group linked through its nitrogen atom to a variety of aromatic, arylalkyl, heteroaromatic, and cycloaliphatic substituents. Finally, some halogen substituents were introduced at position 9. The combination of all these structural modifications led us to prepare more than 400 compounds with the general Structure I, described in part in a

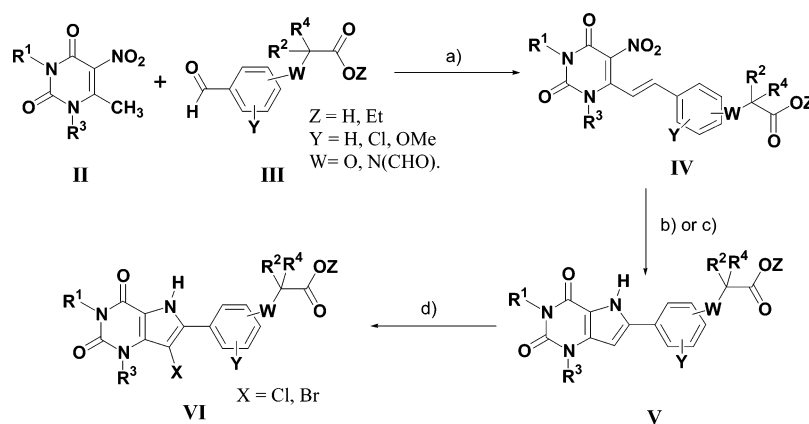
recent patent.³⁶ For the sake of clarity, we decided to publish their preparation and biological tests on AdoRs, SAR, and SSR in three separated articles in this journal.

In the first paper of the series we report on 9-dAXs of Structure I bearing the structural features indicated in Chart 2. In the second article, we will describe and discuss the synthesis and biological activity of cyclic amide derivatives of 9-dAXs prepared from differently functionalized piperidines, piperazines, and tetrahydroisoquinolines. Finally in the third paper we will address quantitative aspects of the structure–affinity relationships (especially at *hA*_{2B} receptors) through traditional QSAR (Hansch approach) and 3D QSAR (GRID/CoMFA-GOLPE) methods, and docking studies of some representative ligands on AdoR subtype models, developed by means of homology building techniques.

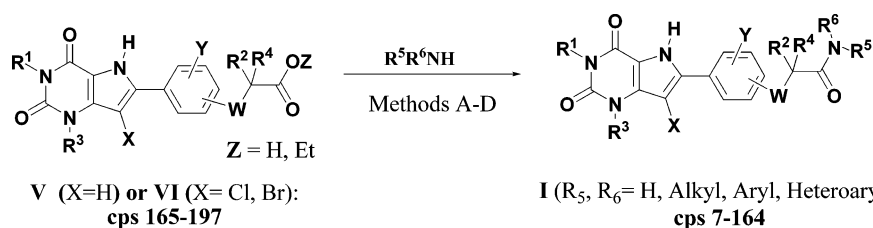
Chemistry. The synthesis of 9-dAX (1,3-dialkyl-8-substituted-1*H*-pyrrolo[3,2-*d*]pyrimidine-2,4(3*H*,5*H*)-diones) derivatives was performed according to published procedures.^{34,37,38} First, the appropriate 6-styryluracils **IV** (Scheme 1) were synthesized by standard methods and then cyclized to the corresponding 9-dAXs **V**. 9-dAXs **V** and their corresponding 9-halogen derivatives **VI** bearing an oxyacetic acid or an oxyacetic ester group (Table 6) on the para position of the 8-phenyl ring were subsequently converted to amides **I** by different methods (Scheme 2, Tables 1–5).

Molecules with chiral centers were isolated and tested as racemic mixtures. Novel 1,3-dialkyl-5-nitro-6-methyluracils **II** (compounds **201–203**, Table 11 in Supporting Information) and benzaldehydes **III**^{39–43} required for the synthesis of 6-styryl derivatives **IV**, were obtained as summarized below.

The 1,3-dialkyl-6-methyluracil precursors of **II**, were prepared as follows: symmetrically substituted ($R^1 = R^3$) 1,3-dialkyl-6-methyluracils were obtained by alkylation of 6-methyl-

Scheme 1^a

^a (a) Dioxane/piperidine/reflux; (b) P(OEt)₃, reflux; (c) Na₂S₂O₄/HCO₂H, reflux; (d) SO₂Cl₂ or Br₂/AcOH.

Scheme 2^a

^a Method A (Z = Et): NaCN/dioxane, reflux/sealed tube. Method B (Z = H): isobutyl chloroformate/NMP/THF. Method C (Z = H): EDC/OHBTf/triethylamine. Method D (Z = H): EDC/OHBTf/polymer bound morpholine/DMF.

(1*H*,3*H*)-pyrimidine-2,4-dione⁴⁴ or by treatment of the appropriate 1,3-disubstituted ureas with acetic anhydride and 4-*N,N*-dimethylaminopyridine.⁴⁵ 1-Alkyl-6-methyluracils were prepared by acetoacetylation of the proper monosubstituted urea followed by cyclocondensation.⁴⁶ 3-Alkyl-6-methyluracils were readily accessed by reaction of monosubstituted ureas with ethyl acetoacetate.^{47,48} Novel nonsymmetrically substituted ($R^1 \neq R^3$) 1,3-dialkyl-6-methyluracils precursor (compounds **198**–**199** in Table 10 and compound **200** in page S3 of Supporting Information) were prepared by selective alkylation at position 3 or 1 of the corresponding 1 or 3 monosubstituted 6-methyluracil with sodium hydride and alkyl iodide.

The synthesis of novel benzaldehydes **III** was performed by alkylation of the sodium salts of the corresponding 4-hydroxybenzaldehyde with the appropriate α -haloester.^{40–44}

3-Chloro-4-formylphenoxyacetic acid **204** was obtained by basic hydrolysis of the ethyl (3-chloro-4-formylphenoxy)acetate.⁴⁰ The synthesis of 4-formylphenylamino acetic acid ethyl ester **205** was performed by alkylation of the alkaline salts of the 4-aminobenzaldehyde⁴⁹ with bromoethyl acetate.

The condensation of the 1,3-dialkyl-6-methyl-5-nitrouracils **II**³³ with the appropriate benzaldehyde **III** in dry dioxane and few drops of piperidine as catalyst allowed us to obtain the corresponding (*E*)-6-styryl derivatives **IV** (compounds **206**–**216**, Scheme 1, Table 12 in Supporting Information) in satisfactory yields.

The ring closure of **IV** to the 9-dAXs **V** (compounds **165**–**170**, **172**, **173**–**188**, and **191**–**197**, Table 6) was performed by reductive cyclization (Scheme 1) using either neat triethyl phosphite (Method A) or sodium dithionite in formic acid (Method B) under reflux. The yields of the cyclization (Table 4 in Supporting Information) were only moderate and highly dependent on the starting 6-styryluracil. In most reactions, sodium dithionite proved to be a superior reagent. Interestingly, in the cyclization with triethyl phosphite, the starting carboxylic acids were transformed into the corresponding ethyl esters, whereas the cyclization employing sodium dithionite in formic acid promoted the oxyacetic ester hydrolysis to the carboxylic acid. Several carboxylic acids **V** ($Z = H$) were also prepared through the hydrolysis of the corresponding ethyl esters ($Z = Et$) (Table 6).

9-Halogeno derivatives **VI** (compounds **171** and **173**: $X = Cl$; **189** and **190**: $X = Br$) were synthesized by using sulfonyl chloride and bromine in acetic acid,⁵⁰ respectively.

Starting from **V** or **VI** (compounds **165**–**197**, Table 6), different methods were applied to prepare amide derivatives **I** (compounds **7**–**164**, Scheme 2, Tables 1–5). The synthetic strategies include the use of both classical synthetic procedures (Methods A–C) and a method (Method D) adapted to medium throughput parallel synthesis.³⁶ The first amidation procedure (Scheme 2, Method A)⁵¹ implies the reaction of the 9-dAXs esters with an excess of the appropriate amine and a catalytic amount of sodium cyanide in dioxane at reflux or under appropriate heating in a sealed tube. A second employed method involved direct condensation of carboxylic acids and the suitable amines in polar aprotic solvents (DMF, tetrahydrofuran) in the presence of an organic base (triethylamine or polymer-supported morpholine) and 1-[3-(dimethylamino)-propyl]-3-ethylcarbodiimide hydrochloride (EDC) and 1-hydroxybenzotriazole (OHBT) (Methods C and D) as coupling reagents. In a third procedure, the carboxylic acids were converted into a mixed anhydride intermediates by treatment with isobutyl chloroformate and *N*-methylmorpholine (NMP) and then reacted with the proper amines (Method B).

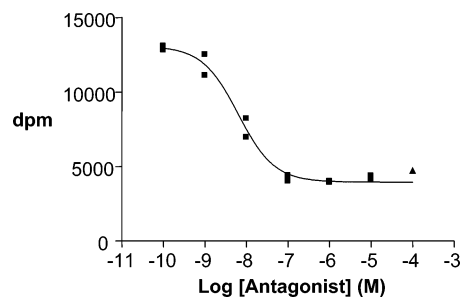


Figure 1. Binding competition experiments at cloned *hA*_{2B} AdoR. A representative example is shown with compound **68** (■). Nonspecific binding was measured with 10⁻³ M NECA (▲). The assay was performed in duplicate.

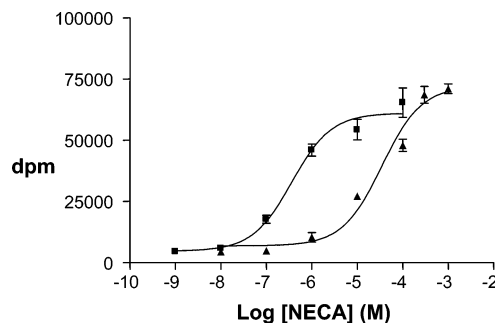


Figure 2. cAMP accumulation experiments. An example is shown with compound **68** at *hA*_{2B} receptors transfected in CHO cells. Cumulative concentration–response curves to NECA in the absence (■) and in the presence (▲) of 0.1 μ M **68**. Each point represents the mean \pm SEM (vertical bars) of triplicate measurements.

Biochemical and Pharmacological Assays. Compounds were tested for their ability to displace [³H]-DPCPX, [³H]-ZM241385, [³H]-DPCPX, and [³H]-NECA from cloned human A₁, A_{2A}, A_{2B}, and A₃ AdoRs (see Table 16 in Supporting Information). All the active compounds showed competition concentration–response curves of specific radioligand binding against increasing concentrations of ligands, the slopes not being significantly different from unity at the 5% level of statistical significance. Assays were carried out by coinubation of compounds, in at least six different concentrations, with the appropriate radioactive ligand. A representative binding competition curve is shown in Figure 1.

The antagonistic activity and efficacy of a number of selected ligands were measured by means of the adenylyl cyclase functional assay at cloned *hA*_{2B} and *hA*_{2A} AdoR subtypes and in isolated organs at both guinea pig A_{2B} and rat A_{2A} AdoR subtypes. All the active compounds concentration-dependently displaced the curves of the NECA AdoR agonist to the right in a parallel way without depression of their maximum, which is the typical behavior of competitive antagonists. Representative examples are shown in Figures 2 and 3 for the experiments on A_{2B} and A_{2A} AdoR subtypes from transfected cells (*hA*_{2B}) and from isolated animal organs, respectively.

The antagonist activity and efficacy of the tested ligands are collected in Table 9.

Results and Discussion

The most exploited class of 9-dAXs was represented by 1,3-symmetrically ($R^1 = R^3$) substituted ligands, that are 1,3-dipropyl and 1,3 dimethyl derivatives (59 and 21 compounds, reported in Tables 1 and 2, respectively). A further series of 1,3-nonsymmetrically ($R^1 \neq R^3$) substituted 9-dAXs AdoR ligands (25 compounds) was prepared for a more complete analysis of the SAR and SSR at the 1,3 positions. As an

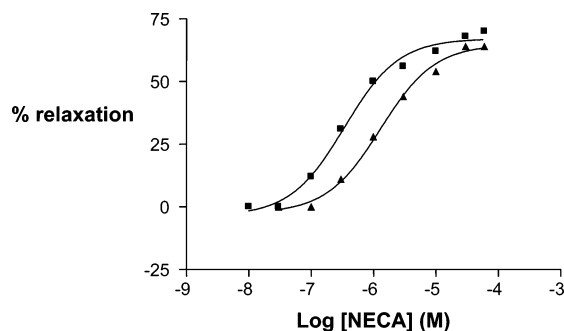


Figure 3. Functional assay. An example is shown with compound **68** at A_{2B} receptors in smooth muscle of guinea pig thoracic aorta. Cumulative concentration–response curves to NECA in the absence (■) and in the presence (▲) of 30 nM **68**.

additional structural modification, methyl, ethyl, and, more rarely, phenyl groups were introduced at the position α to the carbonyl of the oxyacetamido group linking the phenyl ring in 8-position to phenyl or benzyl groups. It must be underlined that these structural modifications led to chiral molecules which were tested as racemic mixtures. The synthesis of selected chiral 9-dAX amides, starting from optically pure enantiomers of 9-dAX acids is now in progress and will be reported in due course. Symmetric α,α -dimethyl ($R^2 = R^4 = \text{CH}_3$, Structure I) substituted ligands were also prepared. To evaluate the importance of an intact, condensed pyrrole in the 9-dAX ring system for the AdoR affinity and selectivity, two additional structural variations were carried out: the methylation of the N7 nitrogen^{33,35} and the halogenation at the C9 with a chloro or bromo atom.³⁶ Moreover, a methoxy group was placed in the ortho or meta-position of the 8-phenyl ring and in one instance also a chloro atom was introduced in the ortho-position.

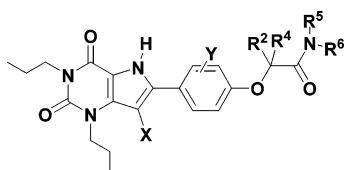
Along with 9-dAX anilides and benzylamides, many heteroaromatic amides were synthesized. Many of them were properly chosen substituted at the aromatic or heteroaromatic amide rings to assess the effects on the affinity and selectivity of steric, electronic, and lipophilic substituent properties. However, we have to remind that the first goal of the present research program was the discovery of new, highly active hA_{2B} antagonists endowed with good hA_{2A}/hA_{2B} affinity ratios (>100) and therefore once that compounds with these characteristics were discovered the affinities for the other two AdoR subtypes, namely hA₁ and hA₃, were measured. According to this strategy, the biological assays were performed up to the determination of the pK_i only for the most promising ligands in the initial screening. In other words, the binding affinities at hA_{2B} and hA_{2A} AdoR were first measured as % of radioligand displacement at 0.1 μM concentration (for the hA_{2B} often also at 0.01 μM) and only when they were indicative of a high hA_{2B} AdoR affinity and a likely high hA_{2B}/hA_{2A} selectivity, the pK_is were determined at both AdoR subtypes. For this reason, for several compounds in Tables 1–6, only the % of radioligand displacement at the indicated concentrations is reported. In this regard, it must be said that for an appropriate evaluation of the SAR the pK_i values were measured also for some informative compounds that did not conform to the requisites described above. Finally, to avoid the loss of important information for the detection of key structural elements responsible for a high or low binding affinity, also the percentages of radioligand displacement at the same concentrations were cautiously compared. They were considered as indicative of a significantly diverse affinity when the radioligand displacement differed for more than 15%. Even if those comparisons had to be made with much precaution, the analysis of a relatively high array of data

in our hand (% of displacements /IC₅₀ /pK_i) made us confident about their acceptable reliability. From the previous discussion it should be evident that the study of the SAR mainly addressed the binding affinity at the hA_{2B} receptor subtype. Occasionally, some SARs at the hA_{2A} receptor subtype were performed for particular classes of ligands. In addition to that, the analysis of the SSRs was also carried out, but at a more qualitative and general level.

For the sake of clarity, the discussion of the SAR and to a lesser extent of the SSR is made here separately for each class of ligands, according to the structural classifications reported in Tables 1–6. In all the tables, the examined ligands are ordered on the basis of their decreasing hA_{2B} affinity, considering first their pK_is, then the % of radioligand displacement at 0.1 μM and finally at 0.01 μM . For a more immediate and efficient analysis of the variation of both affinity and selectivity, the binding data (pK_i) are presented graphically as a plot of pK_i hA_{2A} (Y axis) versus pK_i hA_{2B} (X axis) using the same scale and range for both axes (square plot). On the diagonal of this plot ($Y = X$) there will lie therefore compounds with equal affinities at both receptors, whereas hA_{2B} or hA_{2A} selective compounds will be seen below or above the diagonal, respectively. The distance of their pK_i values from the diagonal is a direct measure of their degree of selectivity. The compounds targeted in the present work, that are those endowed with high hA_{2B} affinity and high hA_{2B}/hA_{2A} selectivity will be therefore located in the lower right-hand side corner of the plots. Whenever possible, a comparative analysis among similarly substituted ligands belonging to diverse classes is made; this analysis has been extended also to the comparison between xanthines and 9-dAXs. Some considerations on the SAR and SSR are presented also for the ester and carboxylic acid intermediates reported in Table 6.

1,3-Dipropyl-8-[4-phenoxy-N-phenylacetamido]-9-deazaxanthines (compounds 7–65). Nearly 60 1,3-dipropyl-8-substituted-9-dAXs were prepared and tested for their binding affinity at hA_{2A} and hA_{2B} receptors (Table 1). pK_i values ranging from 6.14 to 7.92 and from 6.70 to 8.66 were measured for the hA_{2A} and hA_{2B} AdoR, respectively; their relationship and distribution are represented as a plot of pK_i hA_{2B} vs pK_i hA_{2A} in Figure 4. A simple visual inspection of the plot revealed that hA_{2B} and hA_{2A} binding affinities are not correlated and that most of the examined ligands are slightly selective toward the hA_{2B} receptor subtype, with the exception of compound **38** which is a weakly hA_{2A} selective ligand, lying slightly above the diagonal of the plot. Indeed, in the whole series, the $K_i hA_{2A} / K_i hA_{2B}$ selectivity ratios were relatively low, reaching the maximum value of 34.7 with the bulky *p*-OCH₃ phenyl derivative congener **25**, which in the plot of Figure 4 is represented by the point showing the greatest distance from the diagonal.

A further analysis of the $K_i hA_{2A} / K_i hA_{2B}$ affinity ratios indicated that values > 10 ($\Delta pK_i > 1$) were found for eight compounds (occupying in the plot the region below the line [$Y = X - 1$] parallel to the diagonal), bearing in the anilide phenyl ring substituents with quite diverse steric, lipophilic, and electronic properties. Therefore, a clear interpretation of the substituent effects on SSRs cannot be proposed. By contrast, the analysis of the SARs at the hA_{2B} AdoR allowed the identification of the key molecular determinants for a favorable receptor binding. The most active compound at hA_{2B} was the *p*-Br-phenyl derivative **7** with a pK_i = 8.66 and a moderate $K_i hA_{2A} / K_i hA_{2B}$ affinity ratio (14.1). It is important to note that five out of the ten most active ligands at hA_{2B} AdoR

Table 1. Chemical Structures and Binding Affinities at the hA_{2B} and hA_{2A} AdoRs of 1,3-Dipropyl-9-dAX Anilide Ligands 7–65**General Structure of cps 7-65**

compd	X	Y	R ² /R ⁴	R ⁵ /R ⁶	pK _i ^a hA_{2B}	pK _i hA_{2A}	K _i A _{2A} /K _i A _{2B}	hA_{2B} ^a [0.1 μM]	hA_{2B} ^a [0.01 μM]	hA_{2A} ^a [0.1 μM]
7	H	H	H/H	H/C ₆ H ₄ -4Br	8.66	7.51	14.1	97	66	54
8	H	H	H/H	H/C ₆ H ₄ -4Cl	8.50	7.50	20	95	58	61
9	H	H	Me/H	H/C ₆ H ₄ -4F	8.49	7.23	18.2	88	62	51
10	H	H	H/H	H/C ₆ H ₄ -4F	8.48	7.92	3.6	96	70	62
11	H	H	Et/H	H/C ₆ H ₄ -4F	8.32	7.72	4	100	68	88
12	H	H	Me/H	H/C ₆ H ₅	8.29	6.98	20.4	92	50	42
13	H	H	Me/H	H/C ₆ H ₄ -4OMe	8.29	7.41	7.6	92	55	57
14	H	H	Et/H	H/C ₆ H ₄ -4Br	8.22	7.50	5.2	94	55	82
15	H	H	H/H	H/C ₆ H ₄ -4OCF ₃	8.16	6.97	15.5	91	53	31
16	H	H	H/H	H/C ₆ H ₄ -4CH ₂ SO ₂ NC ₄ H ₈	8.11	7.28	6.8	70	58	31
17	H	H	H/H	H/C ₆ H ₄ -4C(Me) ₃	8.10	7.10	10	94	51	47
18	H	H	Me/Me	H/C ₆ H ₅	8.10	7.27	6.8	93	51	57
19	H	H	Me/Me	H/C ₆ H ₄ -4F	8.05	7.77	1.9	97	50	32
20	H	H	H/H	H/C ₆ H ₄ -4OCH ₂ C ₆ H ₅	8.05	7.73	2.1	76	49	60
21	H	H	H/H	H/C ₆ H ₅	8.03	6.65	24	92	47	6
22	H	H	Et/H	H/C ₆ H ₅	8.01	7.59	2.6	93	48	88
23	H	H	H/H	H/C ₆ H ₄ -4CH ₂ CN	7.95	7.40	3.5	86	34	46
24	H	H	H/H	H/C ₆ H ₄ -4OMe	7.92	7.70	1.7	80	22	52
25	H	H	H/H	H/C ₆ H ₄ CONH(CH ₂) ₂ - C ₆ H ₄ -4OMe	7.91	6.37	34.7	74	21	13
26	Br	H	H/H	H/C ₆ H ₄ -4F	7.90	7.70	1.6	72	30	70
27	H	H	H/H	H/C ₆ H ₄ -4NHCOMe	7.86	7.20	4.6	70	23	40
28	H	H	H/H	H/C ₆ H ₄ -4Me	7.85	—	—	81	27	44
29	H	H	H/H	H/C ₆ H ₄ -4C ₆ H ₅	7.79	7.16	4.3	80	40	36
30	H	H	H/H	H/C ₆ H ₄ -4SO ₂ C ₆ H ₅	7.76	6.55	16.2	85	10	27
31	Cl	H	H/H	H/C ₆ H ₄ -4Me	7.73	7.49	1.7	78	38	50
32	H	H	H/H	H/C ₆ H ₄ -2OH	7.72	7.49	1.7	74	56	82
33	H	H	H/H	H/C ₆ H ₄ -4I	7.71	6.80	10	80	30	57
34	H	H	H/H	H/C ₆ H ₄ -4COMe	7.70	—	—	62	24	15
35	Cl	H	H/H	H/C ₆ H ₄ -4Cl	7.64	7.05	3.9	80	17	28
36	Cl	H	H/H	H/C ₆ H ₄ -4Br	7.61	6.90	5.1	73	15	37
37	Br	H	H/H	H/C ₆ H ₅	7.61	7.37	1.7	73	16	54
38	H	H	H/H	H/C ₆ H ₄ -4CONH ₂	7.60	7.62	0.95	78	16	43
39	Cl	H	H/H	H/C ₆ H ₄ -4OMe	7.56	7.35	1.6	70	15	45
40	Cl	H	H/H	H/C ₆ H ₄ -4F	7.56	7.39	1.5	69	10	54
41	H	H	H/H	H/C ₆ H ₄ -4CN	7.48	6.77	5.13	56	11	10
42	H	H	H/H	H/C ₆ H ₄ -4CH ₂ COOH	7.47	6.65	6.6	87	14	28
43	H	H	H/H	H/C ₆ H ₄ -4OH	7.46	7.25	1.6	79	24	51
44	H	H	H/H	H/C ₆ H ₄ -4-R ^c	7.46	7.04	2.6	67	11	25
45	Cl	H	H/H	H/C ₆ H ₅	7.43	7.13	2	57	11	37
46	Cl	H	H/H	H/C ₆ H ₄ -4COMe	7.28	7.07	1.6	43	8	21
47	H	H	H/H	H/C ₆ H ₄ -4COOEt	7.25	7.00	1.8	57	6	30
48	H	H	H/H	H/C ₆ H ₄ -4CH ₂ COOEt	7.22	6.62	4.0	58	32	10
49	Cl	H	H/H	H/C ₆ H ₄ -3F	7.22	6.61	4.1	46	6	20
50	H	H	H/H	H/C ₆ H ₄ -4CHO	7.20	6.31	7.8	67	13	13
51	H	H	H/H	H/C ₆ H ₄ -4COC ₆ H ₅	7.11	—	—	51	11	13
52	Cl	H	H/H	H/C ₆ H ₄ -2Cl	7.08	6.58	3.2	44	5	23
53	H	H	H/H	H/C ₆ H ₄ -4N(Me) ₃	7.04	6.15	7.8	52	4	8
54	Cl	H	H/H	H/C ₆ H ₄ -2F	6.85	6.14	5.1	30	5	2
55	H	H	H/H	H/C ₆ H ₄ -4SO ₂ NH ₂	6.70	—	—	53	10	37
56	H	H	Ph/H	H/C ₆ H ₅	—	—	—	89	44	75
57	H	H	H/H	H/C ₆ H ₃ -2OH,5F	—	—	—	89	29	73
58	H	H	H/H	H/C ₆ H ₃ -2OH,4F	—	—	—	88	23	80
59	H	H	Me/Me	H/C ₆ H ₄ -4Br	—	—	—	87	49	54
60	H	H	H/H	H/C ₆ H ₄ -4CF ₃	—	—	—	85	14	19
61	H	H	Ph/H	H/C ₆ H ₄ -4F	—	—	—	84	32	65
62	H	<i>o</i> -Cl	H/H	H/C ₆ H ₄ -4Br	—	—	—	79	17	31
63	H	<i>o</i> -OMe	H/H	H/C ₆ H ₄ -4Br	—	—	—	64	18	39
64	H	<i>o</i> -OMe	H/H	H/C ₆ H ₄ -4F	—	—	—	27	16	43
65	H	<i>o</i> -OMe	H/H	H/C ₆ H ₅	—	—	—	17	3	35

^a Binding affinity values represent the mean of at least three independent experiments; the SEM (standard mean error) was always lower than 10%.^b Binding affinity is expressed as % of radioligand displacement at the concentrations indicated in square brackets. ^c R = 4,4-dimethyl-4,5-dihydro-1,3-oxazol-2-yl.

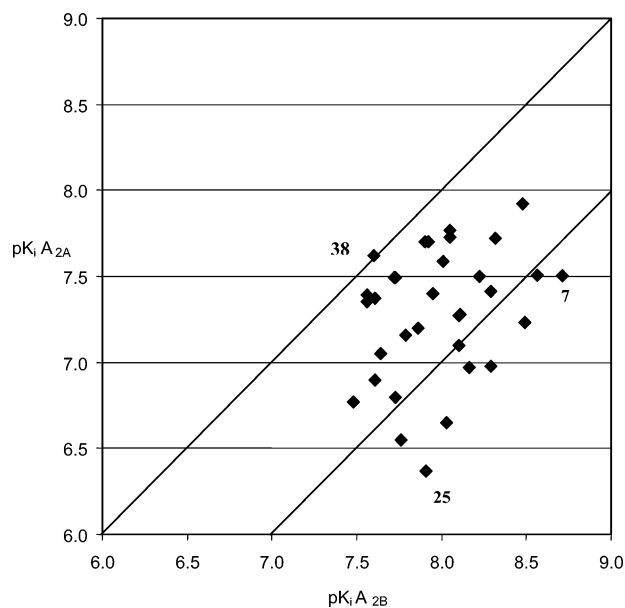


Figure 4. Affinity-selectivity plot for 1,3-dipropyl-9-dAX anilide ligands **7–65** (see Table 1).

are derivatives α -monoalkylated at the oxyacetamido bridge. Some of them, in particular the α -monomethyl derivatives, were even more active and sometimes more hA_{2B} selective than the corresponding parent compounds (**12** vs **21** and **13** vs **24**). α -Ethyl and α,α -dimethyl derivatives displayed at hA_{2B} an activity generally similar or lower than the corresponding not alkylated congeners (**11** vs **10**, **14** vs **7**, **19** vs **10**).

A decrease of hA_{2B} activity could be seen also for the α -phenyl substituted p -F phenyl congeners **61** vs the corresponding unsubstituted derivative **10**.

The change of affinity coming from the introduction of an halogen at position 9 was also explored. Irrespective of the type of halogen used (Cl or Br) and of the parent compound modified, a significant lowering of the activity (from 0.1 to 1.2 log units) was observed at both the hA_2 AdoR subtypes. An even more dramatic drop of activity was detected upon the methylation of the N_7 nitrogen atom [data not shown; Franco Fernandez, University of Santiago de Compostela (personal communication)]. This last finding is in full agreement with previous reports by us³⁵ and others.³³ Two of the most active compounds, i.e., **7** and **10**, and the lead compound **21** were modified by introducing a methoxy group at the ortho-position of the 8-phenyl ring. For the p -Br phenyl derivative **7**, a chloro substituent was also introduced at the ortho position of the 8-phenyl ring (compound **62**). In all instances, and more evidently in the o -OCH₃ congeners **64** and **65**, a strong decrease in activity was recorded.

The substituent effects on the binding affinity at hA_{2B} and hA_{2A} AdoRs were thoroughly explored at the phenyl ring of the aniline moiety, in particular at the para-position. The substituents were chosen in order to properly sample the physicochemical domain of their steric, lipophilic, and electronic properties. An initial analysis of the SARs at the hA_{2B} receptor suggested that the affinity increases as the lipophilicity of the para-substituents increase (compare the lead compound **21** with **15**, **14**, **10**, **8**, and **7**). Lipophilic but bulky substituents such as *t*.But, Ph, I, and OBn (**17**, **29**, **33**, and **20**, respectively) did not produce the expected strong enhancement of affinity, and this might imply that when the substituent overcomes a certain size, a negative steric effect, somehow hindering a favorable hydrophobic interactions, may take place. Finally, a careful analysis

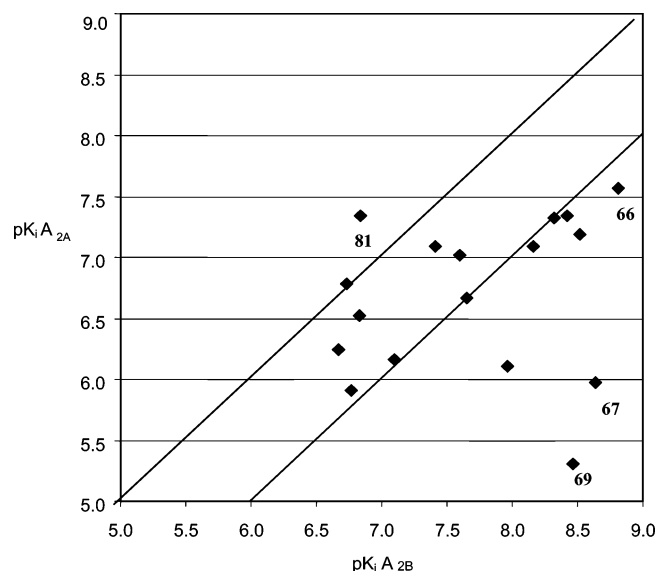


Figure 5. Affinity-selectivity plot for 1,3-dimethyl-8-substituted-9-dAX anilide ligands **66–86** (see Table 2).

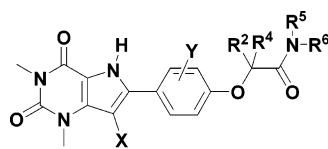
of ligands carrying electron-withdrawing para-substituents pointed out that their affinity increases with the increase of their electron-withdrawing character, regardless of their lipophilic properties.

As far as the SARs at the hA_{2A} receptor are concerned, it is worth to note that the three most active ligands are all p -F phenyl derivatives (**10**, **11**, and **19**) and that the drop of affinity observed at hA_{2B} with the introduction of a halogen in 9-position was confirmed also at the hA_{2A} AdoR. The effect of the substituents of the anilino ring on the affinity at hA_{2A} was not well interpretable as at hA_{2B} .

1,3-Dimethyl-8-[4-phenoxy-*N*-phenylacetamido]-9-deazaxanthines (compounds **66–86).** A limited number of 1,3-dimethyl-8-substituted-9-dAXs were prepared and tested for their binding affinity at hA_{2A} and hA_{2B} AdoRs (Table 2). pK_i values ranging from 5.31 to 7.57 and from 6.67 to 8.81, at the hA_{2A} and hA_{2B} AdoRs, respectively, were measured. The absence of any relationship between the two sets of pK_i s can be easily seen in the plot of $pK_i hA_{2A}$ vs $pK_i hA_{2B}$ of Figure 5. At a first glance it appears that this small series of compounds contains a relatively high number of ligands with a $K_i hA_{2A}/K_i hA_{2B}$ affinity ratio > 10 . They can be easily located in the region of the plot below the line [$Y = X - 1$] parallel to the diagonal. In the same region, in the right-hand side low corner, lies the most potent and selective hA_{2B}/hA_{2A} compound reported in this work, compound **69**. Above the diagonal lies instead compound **81**, a somewhat hA_{2A} selective ligand (3-fold over hA_{2B}) of this series.

The analysis of the chemical structures in Table 2 indicated that only few compounds of this series share a common substitution pattern with compounds of the 1,3-dipropyl series, and therefore no direct comparison among affinity and selectivity data of the two series could be made. Very close activities at hA_{2B} AdoR were observed in the two series for the unsubstituted anilides **21** and **75**, for the p -F-phenyl derivatives **10** and **68** and for the p -Br-phenyl derivatives **7** and **67**. By contrast, the hA_{2B} receptor affinities of the p -COCH₃- (**70**) and p -CN-phenyl- (**71**) 1,3-dimethyl substituted ligands were significantly greater than the corresponding 1,3-dipropyl congeners **34** and **41** (8.45 vs 7.70 and 8.42 vs 7.48, respectively).

Analogous to the 1,3-dipropyl series, the monomethylation at the α -carbon atom of the oxyacetanilide moiety led to higher

Table 2. Chemical Structures and Binding Affinities at the hA_{2B} and hA_{2A} AdoRs of 1,3-Dimethyl-9-dAX Anilide Ligands **66–86****General Structure of cps 66-86**

compd	X	Y	R ² /R ⁴	R ⁵ /R ⁶	pK _i ^a hA_{2B}	pK _i ^a hA_{2A}	K _i A_{2A} /K _i A_{2B}	hA_{2B} ^b [0.1 μM]	hA_{2B} ^b [0.01 μM]	hA_{2A} ^b [0.1 μM]	pK _i ^{a,c} A_1	pK _i ^{a,c} A_3
66	H	H	Me/H	H/C ₆ H ₄ -4Br	8.81	7.57	17.4	93	89	77	—	—
67	H	H	H/H	H/C ₆ H ₄ -4Br	8.58	5.91	741	90	84	12	7.74	8% [1 μM]
68	H	H	H/H	H/C ₆ H ₄ -4F	8.52	7.19	21.3	100	72	41	7.83	20% [1 μM]
69	H	<i>o</i> -OMe	H/H	H/C ₆ H ₄ -4Br	8.46	5.31	1412.5	83	60	20	7.49	4.97
70	H	H	H/H	H/C ₆ H ₄ -4Ac	8.45	—	—	91	65	36	—	—
71	H	H	H/H	H/C ₆ H ₄ -4CN	8.42	7.34	12	91	60	47	8.37	—
72	H	H	Me/H	H/C ₆ H ₄ -4F	8.41	—	—	99	76	70	—	—
73	H	H	Me/H	H/C ₆ H ₅	8.32	7.32	10	99	73	60	8.11	6.04
74	H	H	H/H	H/C ₆ H ₄ -4NO ₂	8.16	7.09	11.7	82	52	30	—	—
75	H	H	H/H	H/C ₆ H ₅	7.96	6.11	70.8	91	44	10	6.62	—
76	H	H	H/H	H/indan-1yl	7.65	6.67	9.5	74	30	20	—	—
77	H	<i>o</i> -OMe	H/H	H/C ₆ H ₄ -4F	7.60	7.02	3.8	63	23	31	—	—
78	H	<i>m</i> -OMe	H/H	H/C ₆ H ₄ -4Br	7.41	7.09	2.1	78	15	32	—	—
79	H	<i>o</i> -OMe	H/H	H/C ₆ H ₅	7.16	5.98	15.1	55	12	13	—	—
80	H	H	H/H	H/- <i>c</i> .C ₅ H ₁₁	7.10	6.16	8.7	57	20	8	—	—
81	H	<i>m</i> -OMe	H/H	H/C ₆ H ₄ -4F	6.84	7.34	0.3	45	10	35	—	—
82	H	<i>m</i> -OMe	H/H	H/C ₆ H ₅	6.83	6.52	2	27	10	20	—	—
83	H	H	H/H	H/CH ₂ CH ₂ NH ₂	6.73	6.78	0.9	34	7	38	—	—
84	H	<i>m</i> -OMe	H/H	H/C ₆ H ₄ -4CN	6.67	6.24	2.7	28	10	5	—	—
85	H	H	H/H	Me/C ₆ H ₅	—	—	—	61	15	0	—	—
86	H	<i>m</i> -OMe	H/H	H/C ₆ H ₄ -4COOEt	—	—	—	47	10	0	—	—

^a Binding affinity values represent the mean of at least three independent experiments; the SEM was always lower than 10%. ^b The binding affinity is expressed as % of radioligand displacement at the concentrations indicated in square brackets. ^c Binding affinity expressed as pK_i or % of ligand displacement at the concentrations indicated in square brackets.

active compounds at hA_{2B} (i.e. compounds **66** > **67** and **73** > **75**), the *p*-Br-phenyl derivative **66** (pK_i = 8.81) being the most active of the whole series. However, unexpectedly, the alpha methylation of the *p*-F derivative **68** afforded compound **72** with a slightly lower affinity.

The N-methylation of the anilide nitrogen of the lead compound **75** afforded compound **85** with a decreased hA_{2B} affinity (61% of radioligand displacement compared to 91%, at 0.1 μM).

Electron-withdrawing groups (i.e., NO₂, F, Br, CN, and COCH₃) in the para-position of the anilide phenyl ring increased the activity of the parent compound **75**, whereas in the series of α-methylated ligands and in the ortho and meta substituted derivatives at the 8-phenyl ring, the enhancement of the binding affinity might be attributed to an increased lipophilicity (**66** > **72** > **73**; **69** > **77** > **79**; **78** > **81** ≥ **82**).

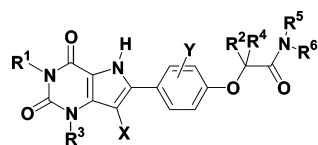
Regarding the hA_{2B}/hA_{2A} selectivity, the most interesting result came from the introduction of a methoxy substituent in the ortho-position of the 8-phenyl ring. While in the parent compound **75** and its *p*-F phenyl derivative **68**, endowed with quite high K_i $hA_{2A}/K_i hA_{2B}$ affinity ratios (71 and 21, respectively), this structural modification determined a marked decrease of both affinity and selectivity (see compounds **79** and **78**), in the *p*-Br phenyl congener **67** the high hA_{2B} activity was maintained whereas an impressive decrease of the hA_{2A} affinity was observed. This ultimately led to a dramatic enhancement of selectivity in compound **69** which was 1412-fold more hA_{2B} over hA_{2A} selective, one of the highest K_i $hA_{2A}/K_i hA_{2B}$ selectivity values reported so far.

This outstanding outcome prompts us to extend the binding assays on **69** also to the other two AdoR subtypes hA_1 and hA_3 . pK_i values of 7.49 and 4.97 for the hA_1 and hA_3 AdoR, respectively, were measured. Therefore, compound **69** could be

considered a high affinity ligand at A_{2B} receptor (K_i = 3.5 nM) with an excellent selectivity over hA_{2A} (K_i $hA_{2A}/K_i hA_{2B}$ = 1412) and hA_3 (K_i $hA_3/K_i hA_{2B}$ = 3090). Unfortunately, the selectivity versus the hA_1 was low (K_i $hA_1/K_i hA_{2B}$ = 9.3), and this calls for further structural modifications aimed at improving this figure while maintaining the excellent selectivities over the other AdoR subtypes. The binding affinities at hA_1 and hA_3 were measured also for the second most selective hA_{2B}/hA_{2A} ligand **67** and for compound **73**, which is the α-methyl derivative of the lead compound **75**. The selectivity pattern observed for **69** was confirmed: the hA_{2B}/hA_1 selectivities remained quite poor, whereas good hA_{2B}/hA_3 selectivities were detected. The hA_{2B}/hA_1 selectivity was determined also for the highly hA_{2B} active *p*-CN phenyl derivative **71**; in this case an even lower hA_{2B}/hA_1 selectivity was measured (K_i ratio close to 1).

Differently from **66**, the introduction of a methoxy group in the meta-position of the 8-phenyl ring of the *p*-F phenyl derivative **68** induced a marked decrease in hA_{2B} affinity leading to compound **81**, one of the few slightly hA_{2A} selective ligands obtained in this work.

Compounds **76**, **80**, and **83**, which are not anilides but differently functionalized *N*-alkyl oxyacetamides, were inserted in Table 2 (1,3-dimethyl-9-dAX derivatives). The indanyl (**76**) and cyclopentyl (**80**) amides showed good affinities at hA_{2B} AdoR with a nearly 10-fold selectivity over hA_{2A} AdoR subtype. Compound **83** was prepared for comparison to its corresponding xanthine derivative, which had been tested several years ago⁵² at the rat A_2 AdoR receptor (at that time the existence of the A_{2A} and A_{2B} receptor subtypes was unknown) and showed a high affinity (pK_i 7.40). Our 9-dAX derivative **83** displays similar affinities at hA_{2B} and hA_{2A} AdoRs (pK_i 6.73 and 6.78, respectively), two values likely lower than in the corresponding xanthine.

Table 3. Chemical Structures and Binding Affinities at the hA_{2B} and hA_{2A} AdoRs of 1,3-Dialkyl of 9-dAX Anilide Ligands 87–111**General Structure of cps 87-111**

Compd	R ¹ /R ³	X	Y	R ² /R ⁴	R ⁵ /R ⁶	pK _i ^{a)}	pK _i ^{a)}	K _i A _{2A} /	hA _{2B} ^{b)}	hA _{2B} ^{b)}	hA _{2A} ^{b)}
						hA _{2B}	hA _{2A}	K _i A _{2B}	[0.1μM]	[0.01μM]	[0.1μM]
87	<i>c</i> .Pr CH ₂ / <i>c</i> .Pr CH ₂	H	H	H/H	H/C ₆ H ₅	8.33	7.81	3.3	96	57	93
88 ^{c)}	Pr/Me	H	H	H/H	H/C ₆ H ₄ -4C ₆ H ₅	8.28	5.58	501	93	39	15
89	Pr/Me	H	H	H/H	H/C ₆ H ₄ -4F	8.25	7.18	11.7	94	57	47
90	Pr/Me	H	H	H/H	H/C ₆ H ₄ -4I	8.23	—	—	97	51	24
91	Et/Et	H	H	H/H	H/C ₆ H ₅	8.11	6.73	24	91	45	22
92	Me/Pr	H	H	H/H	H/C ₆ H ₄ -4F	8.02	6.95	11.7	93	43	24
93	Pr/Me	H	H	H/H	H/C ₆ H ₄ -4COOEt	7.93	5.58	224	88	12	9
94	Pr/Me	H	H	H/H	H/C ₆ H ₅	7.91	6.77	13.8	91	38	18
95	Et/Et	H	H	H/H	H/C ₆ H ₄ -4CN	7.87	6.92	8.91	79	20	2
96	Me/MeOPr	H	H	H/H	H/C ₆ H ₅	7.86	6.92	8.7	80	27	29
97	Me/Pr	H	H	H/H	H/C ₆ H ₅	7.67	6.71	9.1	80	33	40
98	Pr/Me	H	H	H/H	H/C ₆ H ₄ -4CH ₂ COOEt	6.88	—	—	35	10	0
99	Me/MeOPr	H	H	H/H	H/ <i>c</i> .C ₃ H ₉	6.58	6.37	1.6	16	8	0
100	<i>c</i> .Pr CH ₂ / <i>c</i> .PrCH ₂	H	H	H/H	H/C ₆ H ₄ -4F	—	—	—	95	57	98
101	<i>c</i> .Pr CH ₂ / <i>c</i> .PrCH ₂	H	H	H/H	H/C ₆ H ₄ -4Br	—	—	—	94	43	89
102	MeOPr/MeOPr	H	H	H/H	H/C ₆ H ₄ -4Br	—	—	—	85	45	30
103	Me/Pr	H	H	H/H	H/C ₆ H ₄ -4Br	—	—	—	84	—	91
104	CF ₃ CH ₂ /CF ₃ CH ₂	H	H	H/H	H/C ₆ H ₄ -4Br	—	—	—	79	29	11
105	MeOPr/MeOPr	H	H	H/H	H/C ₆ H ₄ -4F	—	—	—	68	24	20
106	CF ₃ CH ₂ /CF ₃ CH ₂	H	H	H/H	H/C ₆ H ₄ -4F	—	—	—	68	22	18
107	MeOPr/MeOPr	H	H	H/H	H/C ₆ H ₅	—	—	—	65	1	28
108	CF ₃ CH ₂ /CF ₃ CH ₂	H	H	H/H	H/C ₆ H ₅	—	—	—	57	15	4
109	<i>i</i> -Bu/Me	H	H	H/H	H/C ₆ H ₅	—	—	—	57	15	2
110	Me/Pr	H	H	H/H	H/ 1-oxo-indan-5-yl	—	—	—	50	12	26
111	Me/ 	H	H	H/H	H/C ₆ H ₄ -4F	—	—	—	27	16	10

^a Binding affinity values represent the mean of at least three independent experiments; the SEM was always lower than 10%. ^b Binding affinity is expressed as % of radioligand displacement at the concentrations indicated in square brackets. ^c pK_i hA₁ = 7.96; pK_i hA₃ = 4.91.

1,3-Dialkyl-8-(phen-4-oxy-*N*-phenylacetamido)-9-deaza-xanthines (compounds 87–111). Along with 1,3-dimethyl- and 1,3-dipropyl-9-dAXs, a number of 1,3-symmetrically (R¹ = R³) and nonsymmetrically (R¹ ≠ R³) alkyl substituted congeners were designed, prepared, and tested. Their chemical structures and binding affinities at hA_{2A} and hA_{2B} AdoRs are reported in Table 3. The 1,3-symmetrically substituted 9-dAXs comprised

ethyl, cyclopropylmethyl, trifluoroethyl, and 3-methoxypropyl derivatives whereas the nonsymmetrically substituted ones included 1-methyl, 3-propyl, 1-methyl-3-(3-morpholin-4-propyl), 1-isobutyl-3-methyl, and 1-propyl-3-methyl derivatives. pK_is were measured only for those ligands whose % of radioligand displacement at hA_{2B} and hA_{2A} AdoR subtypes could have been predictive of a high hA_{2B} affinity and/or high K_ihA_{2A}/ K_ihA_{2B}

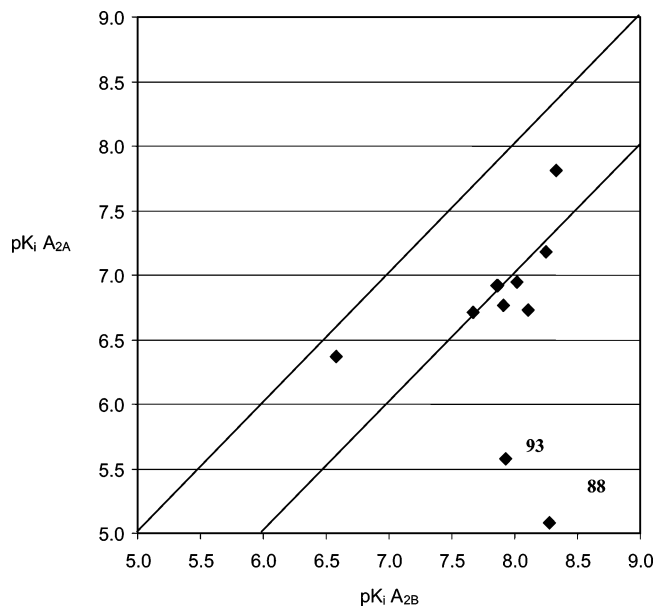


Figure 6. Affinity-selectivity plot for 1,3-dialkyl-9-dAX anilide ligands **87–111** (see Table 3).

affinity ratio. Several ligands with good hA_{2B} affinity (pK_i up to 8.33) and high $K_i hA_{2A}/K_i hA_{2B}$ affinity ratios were obtained as can be seen in the plot of Figure 6.

The plot of pK_i s in Figure 6 suggested that also for this class of AdoR ligands there was no correlation between hA_{2A} and hA_{2B} affinities and that two compounds, occupying the lower right-hand corner of the plot, had a good hA_{2B} affinity and high hA_{2B}/hA_{2A} selectivity. These compounds are both 1-propyl-3-methyl congeners: the *p*-biphenyl derivative **88** ($pK_i hA_{2B} = 8.28$; $K_i hA_{2A}/K_i hA_{2B}$ ratio = 501) and the *p*-COOEt derivative **93** ($pK_i hA_{2B} = 7.93$; $K_i hA_{2A}/K_i hA_{2B}$ ratio = 224).

From a structural point of view, this high selectivity stems from the presence of a bulky group in the para-position of the 8-phenyl ring which seems to be well accepted into the hA_{2B} receptor binding site but not tolerated into the binding regions of hA_{2A} AdoR. Indeed, the observed high selectivity of ligands **88**, **93** mainly originates from their very low affinity toward the hA_{2A} AdoR subtype. A dramatic drop of hA_{2A} affinity was not observed in the most thoroughly explored class of 1,3-dipropyl derivatives bearing the same, or even bulkier, substituents in the para position. This might suggest that a strong steric interaction takes place only at the hA_{2A} AdoR binding sites likely because a quite specific binding of the propyl group in the position 3 and/or the methyl group in position 1 would force the bulky para substituents in a forbidden region. Evidently, this does not apply to the two propyl groups at the positions 1, 3 that, most likely, might be anchored in such a way that the para bulky substituents of the 8-phenyl ring are not placed in sterically hindered receptor regions. This hypothesis could be supported by a docking study of suitably selected para-substituted 1,3-dialkyl ligands into the antagonist binding site of the hA_{2A} AdoR subtype, built by homology modeling.

The excellent hA_{2B} affinity and $K_i hA_{2A}/K_i hA_{2B}$ selectivity of compound **88** prompted us to measure its affinity also at the other two AdoR subtypes hA_1 and hA_3 . While for the latter a very low affinity was detected ($pK_i = 5.91$), for the former a good affinity was observed ($pK_i = 7.96$). Similarly to compound **68**, **88** also presented excellent hA_{2B} affinity, high hA_{2B}/hA_3 selectivity but a still too low selectivity ratio ($K_i hA_{2A}/K_i hA_{2B} = 2.1$).

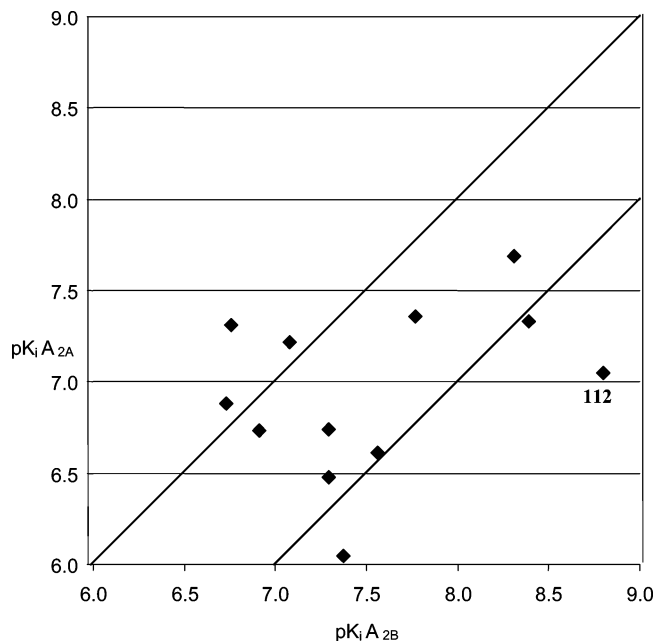


Figure 7. Affinity-selectivity plot for 1,3-dialkyl-9dAX benzamide ligands **112–131** (see Table 4).

The only *N*-alkylamide examined, i.e., the cyclopentylamide **99**, was a 1-methyl-3-methoxypropyl derivative. Its affinity at hA_{2B} ($pK_i = 6.58$) and $K_i hA_{2A}/K_i hA_{2B}$ affinity ratio (1.6) were much lower than the anilide **96** (corresponding values were 7.86 and 8.7, respectively) despite their close lipophilicity.

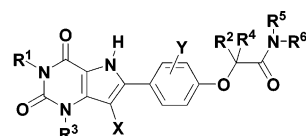
A comparison of the hA_{2B} affinity data among the 1,3-disubstituted parent compounds reported in Tables 1–3 revealed the following decreasing order of affinity at hA_{2B} AdoR: 1,3-dicyclopropylmethyl (**87**) > 1,3-diethyl (**91**) > 1,3-dipropyl (**21**) > 1,3-dimethyl (**75**) > 1-propyl-3-methyl (**94**) > 1-methyl-3-(3-methoxypropyl) (**96**) > 1-methyl-3-propyl (**97**) > 1,3-di-3-methoxypropyl (**107**) > 1,3-ditrifluoroethyl (**108**), and 1-iso-butyl-3-methyl (**109**). This rank of affinity should help the design of high affinity hA_{2B} ligands.

1,3-Dialkyl 8-[phen-4-oxy-(*N*-benzyl)-acetamido]-9-deaza-xanthines (compounds 112–131). Twenty 1,3-dialkyl benzylamide derivatives of 9-dAX were designed, prepared, and evaluated for their affinity at hA_{2B} and hA_{2A} receptors. Ligands with good hA_{2B} affinity (pK_i up to 8.50) and some hA_{2B}/hA_{2A} selectivity were obtained (Table 4).

The plot of $pK_i hA_{2B}$ vs $pK_i hA_{2A}$ in Figure 7 demonstrates that no correlation exist between the two sets of pK_i s and that a number of ligands displayed a $K_i hA_{2A}/K_i hA_{2B}$ affinity ratio nearly to or higher than 10. Considerably lower affinities at hA_{2B} receptors were generally observed in the benzylamide series compared to the corresponding anilide analogues.

An exception to that was the 1,3-dipropyl lead compound **112** whose affinity at hA_{2B} AdoR subtype was consistently higher than the corresponding anilide derivative **21** ($pK_i hA_{2B}$ 8.50 vs 8.03). Notably, the 1,3-dipropyl lead compound **112** presented the highest hA_{2B} affinity and hA_{2B}/hA_{2A} selectivity of the whole series of benzylamides.

Within the series, the hA_{2B} binding affinity of the three lead compounds, that are the 1,3-dipropyl (**112**), 1,3-dimethyl (**119**), and 1-methyl-3-propyl (**131**) benzylamide derivatives, was ranked as follows: **112** > **119** >> **131**. As in the most explored series of 1,3-dimethyl derivatives, the binding affinity strongly increased as the lipophilic character of the para-substituent in the benzyl ring increases (**114** > **115** > **119**). The *N*-alkylation of the benzylamino group did not change significantly the hA_{2B}

Table 4. Chemical Structures and Binding Affinity at the hA_{2B} and hA_{2A} AdoRs of 9-dAX Benzylamide Ligands **112–131****General Structure of cps 112-131**

compd	R ¹ /R ³	X	Y	R ² /R ⁴	R ⁵ /R ⁶	pK _i ^a hA _{2B}	pK _i ^a hA _{2A}	K _i A _{2A} /K _i A _{2B}	hA _{2B} ^a [0.1 μM]	hA _{2B} ^a [0.01 μM]	hA _{2A} ^a [0.1 μM]
112	Pr/Pr	H	H	H/H	H/CH ₂ C ₆ H ₅	8.50	7.05	56.2	95	78	38
113	Pr/Pr	H	H	Me/H	H/CH ₂ C ₆ H ₄ -4Cl	8.39	7.33	11.5	94	55	57
114	Me/Me	H	H	H/H	H/CH ₂ C ₆ H ₄ -4Cl	8.31	7.69	4.2	93	61	75
115	Me/Me	H	H	H/H	H/CH ₂ C ₆ H ₄ -4F	7.77	7.36	2.6	95	36	56
116	Pr/Me	H	H	H/H	H/CH ₂ C ₆ H ₄ -4Cl	7.69	—	—	76	33	20
117	Me/Me	H	H	H/H	H/CH(Me)C ₆ H ₅	7.56	6.61	8.9	63	20	13
118	Me/Me	H	H	H/H	Et/CH ₂ C ₆ H ₅	7.37	6.05	20.9	59	15	17
119	Me/Me	H	H	H/H	H/CH ₂ C ₆ H ₅	7.29	6.74	3.6	66	12	25
120	Me/Me	H	H	H/H	H/CH ₂ C ₆ H ₄ -3OMe	7.29	6.48	6.5	61	15	11
121	Me/Me	H	H	H/H	Me/CH ₂ C ₆ H ₅	7.26	5.99	18.6	67	10	14
122	Pr/Pr	Cl	H	H/H	H/CH ₂ C ₆ H ₅	7.08	7.22	0.7	47	10	43
123	Me/Me	H	<i>o</i> -OMe	H/H	H/CH ₂ C ₆ H ₄ -4Cl	6.91	6.73	1.5	46	11	23
124	Pr/Pr	Cl	H	H/H	H/CH ₂ C ₆ H ₄ -4F	6.76	7.31	0.3	25	8	44
125	Me/Me	H	<i>m</i> -OMe	H/H	H/CH ₂ C ₆ H ₄ -4Cl	6.73	6.80	0.7	43	5	23
126	Pr/Pr	H	H	H/H	H/CH(CH ₂ OH)C ₆ H ₅	—	—	—	77	30	53
127	Pr/Pr	H	H	H/H	H/CH(CH ₂ Cl)C ₆ H ₅	—	—	—	74	25	75
128	Pr/Pr	H	H	H/H	H/CH(COOMe)C ₆ H ₅	—	—	—	58	29	39
129	Pr/Pr	H	H	H/H	H/CH(COOH)C ₆ H ₅	—	—	—	45	38	3
130	Me/Pr	H	H	H/H	Me/CH ₂ C ₆ H ₅	—	—	—	32	15	15
131	Me/Pr	H	H	H/H	H/CH ₂ C ₆ H ₅	—	—	—	21	10	19

^aBinding affinity values represent the mean of at least three independent experiments; the SEM was always lower than 10%. ^bThe binding affinity is expressed as % of radioligand displacement at the concentrations indicated in square brackets.

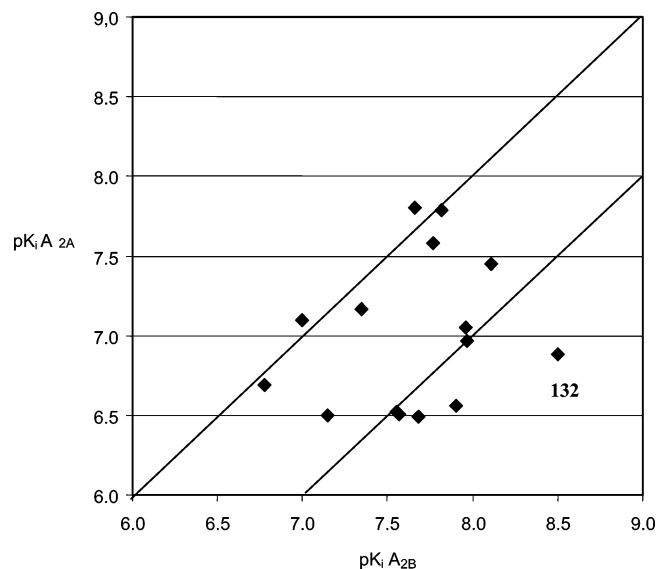
affinity (**119** vs **118** and **121**) but the $K_i hA_{2A}/K_i hA_{2B}$ affinity ratio was enhanced, leading to the two highest hA_{2B} selective compounds of the series (**118**, 20.9, and **121**, 18.6). Methylation of the benzylic carbon of the 1,3-dipropyl lead compound **119** afforded **117** which displayed an enhanced hA_{2B} affinity (pK_i 7.56 vs 7.29). Finally, the introduction of a methoxy group either in the ortho- or meta-position of the 8-phenyl ring of **119** afforded less active ligands (compare **114** vs **123** and **125**).

Replacing the phenyl ring of the benzyl group in the lead compound **119** with the isosteric 4-pyridyl group (see Table 5) led to a likely less active compound **159** (compare the % of displacement at 0.1 μM). A similar behavior was observed for the 1,3-dipropyl lead compound **112**: its 4-pyridyl isoster **143** (see Table 5) shows lower hA_{2B} affinity (7.55 vs 8.50).

Two 1,3-dipropyl-9-chloro derivatives (**122** and **124**) were also prepared. Along with the *m*-methoxy congener **125** they presented a slightly inverted selectivity ($K_i hA_{2A}/K_i hA_{2B}$ ratio < 1). All these three derivatives can be easily detected in the plot of Figure 7 as the points lying above the diagonal. As already observed for other classes of dAXs, the introduction of a halogen in position 9 determined a dramatic decrease of the hA_{2B} activity: pK_i 8.50 vs 7.08 for **112** and **122**, respectively,

Miscellaneous 9-dAX Derivatives (compounds 132–164). A wide range of AdoR ligands with some peculiar structural features were also synthesized and tested (Table 5). They comprised mainly amides of heterocyclic amines (20 compounds), heterocyclic isosteres of benzylamides (**143**, **145**, **159**, and **161**), and finally *N*-formylanilino (**133**, **148**, and **162**) and uracil carbamic acid (**141** and **146**) derivatives. The majority of these compounds should have improved water solubility and, hopefully, a better bioavailability compared to the corresponding anilides and benzylamides.

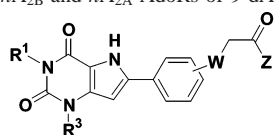
For the reasons discussed in a preceding chapter, for most of these AdoR ligands only the % of radioligand displacements at the two indicated concentrations was determined at both hA_{2A}

**Figure 8.** Affinity–selectivity plot for the miscellaneous 9-dAX derivatives **132–164** (see Table 5).

and hA_{2B} AdoR subtype. Therefore, the SAR and SSR analyses are less robust than those coming from the classes of ligands examined in previous chapter.

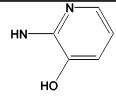
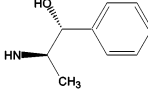
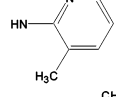
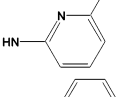
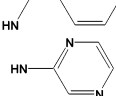
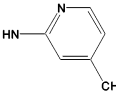
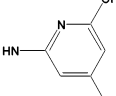
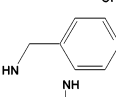
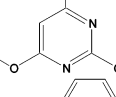
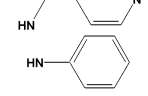
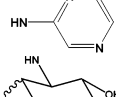
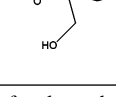
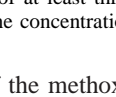
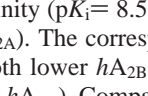
The plot in Figure 8 shows the hA_{2A} and hA_{2B} pK_i variation and distribution and indicates that no relationship exists between the two sets of affinity data. Moreover, only two compounds (i.e. **132** and **136**) have a >20-fold selectivity over the hA_{2B} receptor subtype. Two ligands, which lie just above the diagonal of the plot have an inverted selectivity ($K_i hA_{2A}/K_i hA_{2B}$ affinity ratio < 1). Interestingly, they are both carbamic acid derivatives (**141** and **146**).

One of the most interesting compound in Table 5 was the 1-propyl-3-methyl derivative **132** which presented a 6-OCH₃-

Table 5. Chemical Structures and Binding Affinities at the hA_{2B} and hA_{2A} AdoRs of 9-dAX Ligands 132–164**General Structure of cps 132-164**

Compd	R ¹ /R ³	W	Z	pK _i ^{a)}		K _i A _{2A} / K _i A _{2B}	hA _{2B} ^{b)} [0.1μM]	hA _{2B} ^{b)} [0.01μM]	hA _{2A} ^{b)} [0.1μM]
				hA _{2B}	hA _{2A}				
132	Pr/Me	4-O-		8.50	6.88	41.7	99	57	30
133	Pr/Pr	4-N(CHO)-		8.11	7.45	4.6	93	48	90
134	Pr/Pr	4-O-		7.97	6.97	10	84	41	50
135	Pr/Pr	4-O-		7.96	7.05	8.1	80	30	41
136	Pr/Pr	4-O-		7.90	6.56	21.9	85	40	29
137	Me/Me	4-O-		7.82	7.79	1.1	81	36	43
138	Pr/Pr	4-O-		7.77	7.58	1.5	83	30	65
139	Me/Me	4-O-		7.70	—	—	80	24	34
140	Pr/Pr	4-O-		7.68	6.49	15.5	82	37	32
141	Pr/Pr	4-O-		7.66	7.80	0.7	66	21	76
142	Pr/Pr	4-O-		7.57	6.51	11.5	83	33	34
143	Pr/Pr	4-O-		7.55	6.52	10.7	76	21	18
144	Me/Me	3-O-		7.35	7.17	1.5	73	15	45
145	Me/Me	4-O-		7.15	6.50	4.5	52	10	13
146	Pr/Pr	4-O-		7.00	7.10	0.8	59	24	61
147	Me/Me	3-O-		6.78	6.69	1.2	35	10	32
148	Pr/Pr	4-N(CHO)-		—	—	—	93	24	89
149	Pr/Pr	4-O-		—	—	—	83	19	48
150	Pr/Me	4-O-		—	—	—	73	24	12

Table 5 (Continued)

Compd	R ¹ /R ³	W	Z	pK _i ^{a)}	pK _i ^{a)}	K _i A _{2A} /	hA _{2B} ^{b)}	hA _{2B} ^{b)}	hA _{2A} ^{b)}
				hA _{2B}	hA _{2A}	K _i A _{2B}	[0.1 μM]	[0.01 μM]	[0.1 μM]
151	Pr/Me	4-O-		—	—	—	71	31	22
152	Pr/Pr	4-O-		—	—	—	70	14	18
153	Pr/Me	4-O-		—	—	—	68	25	26
154	Pr/Pr	4-O-		—	—	—	68	20	45
155	Pr/Pr	4-O-		—	—	—	68	17	18
156	Pr/Pr	4-O-		—	—	—	68	10	34
157	Pr/Pr	4-O-		—	—	—	60	25	34
158	Pr/Pr	4-O-		—	—	—	53	12	27
159	Me/Me	4-O-		—	—	—	51	5	37
160	Me/Me	4-O-		—	—	—	50	12	14
161	Pr/Me	4-O-		—	—	—	49	27	3
162	Pr/Pr	4-N(CHO)-		—	—	—	46	10	61
163	Me/Me	4-O-		—	—	—	44	11	20
164	Me/Me	4-O-		—	—	—	33	7	13

^a Binding affinity values represent the mean of at least three independent experiments with a SEM always lower than 10%. ^b The binding affinity is expressed as % of radioligand displacement at the concentrations indicated in square brackets.

3-pyridyl substituent as a replacement of the methoxy phenyl group. Ligand **132** shows high *hA*_{2B} affinity (*pK*_i = 8.50) and a good *hA*_{2B} selectivity (42-fold over *hA*_{2A}). The corresponding 1,3-dipropyl analogue **134** displayed both lower *hA*_{2B} affinity (*pK*_i = 7.97) and selectivity (8-fold over *hA*_{2A}). Comparing the % of displacements at 0.1 μmol of the simple 1,3-dipropyl-3-pyridyl derivative **149**, at *hA*_{2B} and *hA*_{2A} AdoR subtypes, an *hA*_{2B} affinity very close to that determined for the anilidic analogue **21** (83 vs 92%) was observed, whereas the *hA*_{2A} affinity was definitely higher (48% vs 6%).

For the series of ligands, which are heterocyclic isosteres of anilides or benzylamides, we ranked their binding affinities and, whenever possible, made a direct affinity comparison with the corresponding anilides and benzylamides. The affinities at both *hA*_{2A} and *hA*_{2B} AdoR subtypes of the unsubstituted 2- (**142**)

and 3-pyridyl (**149**) derivatives were quite close whereas significant differences were observed for substituted pyridyl congeners. The highest *hA*_{2B} affinities were displayed by the 6-methoxy and 6-methyl-3-pyridyl derivatives (**134** and **136**, respectively) whereas a close (*hA*_{2B}) and a lower (*hA*_{2A}) activity emerged considering the % of radioligand displacements of the 4- and 6-methyl-2-pyridyl isomeric derivatives **150** and **153**, respectively.

When the *hA*_{2B} affinities of the heterocyclic amides were compared with the corresponding isosteric anilides or benzylamides, close or higher affinities were always seen for the latter, i.e., **24** ≅ **134**; **28** ≅ **136**, **32** ≅ **140**; **21** > **142**, **149**, **112** > **143**, **119** > **145**; **21** > **156**.

The 1,3-dipropyl-2',6'-dimethoxy-4'-pyrimidinylamide **135** was endowed with a biological activity nearly identical to the

6'-methoxy-3'-pyridyl congener **134**. The corresponding 1,3-dimethyl analogue of the latter (**160**) showed a lower affinity at both receptor subtypes according to its % of radioligand displacement at 0.1 μM . The same results came from the comparison of the 1,3-dipropyl and 1,3-dimethyl 2'-pyrazinyl amides **156** and **163**, respectively. The 1,3-dimethyl-benzimidazolyl derivative **139** and the 1,3-dipropyl-3'-amino-pyrazolyl derivative **138** showed comparable hA_{2B} affinities, relatively close to those of the parent anilidic compounds **75** and **21**.

The unexpected formylation of the *p*-amino substituent of the 8-phenyl ring during the cyclization reaction of some nitrostyryluracil intermediates with sodium dithionite in formic acid afforded compounds **148** and **162**, whose affinities at hA_{2B} AdoR were close to or lower, for the second, than the affinities observed for the corresponding nonformylated analogues **10** and **21**, respectively. The comparison of the hA_{2A} affinity indicated higher % of radioligand displacement for the formylated derivative, and therefore a lower hA_{2B}/hA_{2A} selectivity could be hypothesized. The other unexpectedly obtained uracil carbamic acid derivatives **141** and **146**, that differ at the N3 substituent (H and CH_3 , respectively) and are ketonic and not amidic derivatives, showed interesting hA_{2A} and hA_{2B} affinities and an inverted selectivity profile, resulting, respectively, in 5- and 6-fold more hA_{2A} selectivity over the hA_{2B} AdoR.

Finally, 1,3-dimethylanilino derivatives **144** and **147**, meta positional isomers of the para-substituted congeners **67** and **75**, respectively, were prepared to evaluate the influence of the anchoring position of the oxyacetamido chain on the affinity and selectivity.

Lower hA_{2B} affinities were observed for meta positional isomers **144** and **147** (7.35 vs 8.58 and 6.78 vs 7.96, respectively) which showed also much lower $K_i hA_{2A}/K_i hA_{2B}$ affinity ratio (1.5 vs 74; 1.2 vs 71 respectively)

Compound **164**, which is a 2-D-glucosamide derivative, was prepared, aiming at a drastically improvement of the water solubility. Unfortunately, very low affinities resulted at both receptor subtypes.

Acid and Ester Intermediates (compounds 165–197). A number of acid and ester intermediates (Structures V and VI, Scheme 1) prepared for the synthesis of 9-dAXs were tested for their binding affinity at hA_{2A} and hA_{2B} AdoR subtypes. The results are listed in Table 6 and reported in graphical form in Figure 9.

From the plot in Figure 9, it is evident that no correlation exists between hA_{2A} and hA_{2B} affinities and that in line with our previous observations, acid and ester intermediates also displayed some selectivity for the hA_{2B} receptor subtypes. The most hA_{2B} active ligand was the 1,3-dipropyl derivative **165** whereas the most selective was **166** with a $K_i hA_{2A}/K_i hA_{2B}$ affinity ratio equal to 93.3. Good selectivities were also displayed by ligands **174** and **172**. Notably the most hA_{2B} selective ligand **166** also showed one of the highest binding affinity at the same receptor ($pK_i = 7.36$).

The observed rank of binding affinities of the acid lead intermediates, for which the pK_i on hA_{2B} were measured, was as follows:

1,3-dipropyl (**165**) > 1-propyl-3-methyl (**166**) = 1-methyl-3-propyl (**167**) > 1-ethyl-3-(3-methoxypropyl) (**170**) > 1,3-dimethyl (**172**) > 1-methyl-3-(3-methoxypropyl) (**174**).

The introduction of a methoxy group in either the ortho- or meta-position of the 8-phenyl ring yielded a lower affinity (compare **172** vs **175** and **179**). The introduction of bromo substituent at position 9 in **165** led to a significant diminution of affinity (see compounds **171** vs **172**).

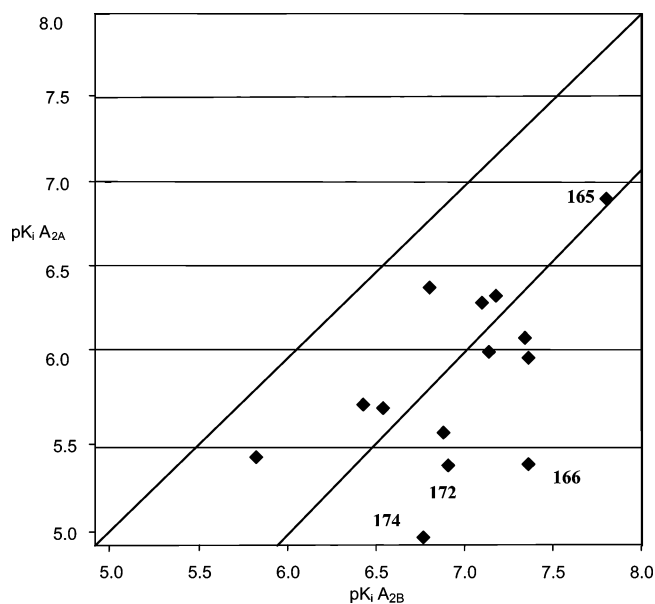


Figure 9. Affinity–selectivity plot for acid and ester intermediates **165–197** (see Table 6).

For only five ethyl esters was the pK_i at both hA_2 AdoR receptor subtypes measured. The most active was the 1-ethyl-3-(3-methoxypropyl) derivative **169** ($pK_i = 7.18$).

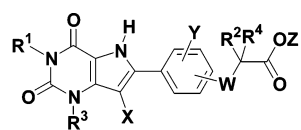
A comparison among acids and the corresponding ethyl esters always indicated a higher hA_{2B} affinity for the former (i.e. **172** > **176**; **174** > **177**; **175** > **178**, **179** > **180**).

Comparison of AdoR Binding Affinities and Selectivities of 9-dAXs with Xanthines. To gain more general insights on the SAR and SSR of AdoR ligands, the affinity and selectivity data of the 9-dAXs reported herein were compared with literature data^{8,18} of xanthine analogues having the same substitution pattern. It must be noted that such a comparison has to be made with caution since the experimental methods used to measure the binding affinity at the different AdoR subtypes were not exactly the same. Indeed, some significant discrepancies between our and Jacobson's data were observed for some xanthine derivatives, reperepared by us as reference compounds (see footnotes in Table 7).

Only a relatively low number of 9-dAXs showed the same substitution pattern of already published xanthines. Therefore, only the AdoR binding affinities of compounds **7**, **8**, **9**, **21**, **28**, **33**, **41**, **112**, and **165** could be compared with those reported for their corresponding xanthines.¹⁸ As far as the binding affinities of xanthines and 9-dAXs at hA_{2B} is concerned, no clear relationship emerged whereas a higher hA_{2B} over hA_{2A} selectivity was almost always observed for xanthines. These results were not confirmed, taking into account the data determined in our assay (see hA_{2B} and hA_{2A} affinity data reported in footnote c of Table 7).

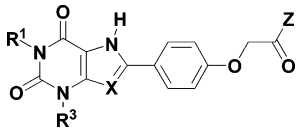
It must be reminded that the heterocyclic systems of xanthines and 9-dAXs, formally differing from the presence–absence of a nitrogen atom at the 9-position, may present greatly diverse physicochemical properties especially in terms of electronic characteristics, ability to make hydrogen bonds, water solubility, and partitions in polar/apolar immiscible solvents.³⁵ These significant differences might result, as our data seem to suggest, in diverse pharmacodynamic (and pharmacokinetic) profiles even when xanthines and 9-dAX derivatives with closely related structures are compared.

The AdoR binding affinities of some 9-dAXs were also compared to those recently published¹¹ for corresponding 8-pyrazolyl, -pyridazinyl, and -pyridyl derivatives (Table 8).

Table 6. Chemical Structures and Binding Affinity at the hA_{2B} and hA_{2A} AdoRs of Acid and Ester Intermediates 165–197**General Structure of cps 165-197**

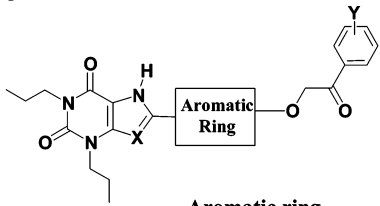
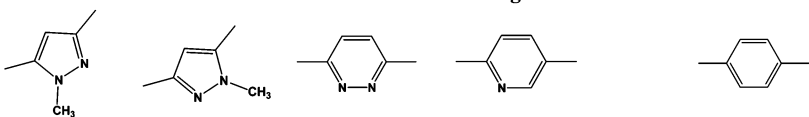
Compd	R ¹ /R ³	X	Y	W	R ² /R ⁴	Z	pK _i ^{a)}		K _i A _{2A} /	hA _{2B} ^{b)}		
							hA _{2B}	hA _{2A}		K _i A _{2B}	[0.1 μM]	[0.01 μM]
165	Pr/Pr	H	H	4-O-	H/H	H	7.80	6.91	8	—	—	—
166	Pr/Me	H	H	4-O-	H/H	H	7.36	5.39	93.3	63	—	21
167	Pr/Pr	H	H	4-O-	Me/H	H	7.36	6.00	22.9	44	—	8
168	Me/Pr	H	H	4-O-	H/H	H	7.34	6.11	17	51	—	15
169	Et/MeOPr	H	H	4-O-	H/H	Et	7.18	6.35	6.8	57	—	16
170	Et/MeOPr	H	H	4-O-	H/H	H	7.14	6.03	12.9	66	—	20
171	Pr/Pr	Br	H	4-O-	H/H	H	7.10	6.31	6.2	48	—	11
172	Me/Me	H	H	4-O-	H/H	H	6.91	5.38	33.9	47	—	14
173	Pr/Pr	Cl	H	4-O-	H/H	H	6.80	6.40	2.5	36	—	19
174	Me/MeOPr	H	H	4-O-	H/H	H	6.67	4.94	53.7	35	—	11
175	Me/Me	H	<i>m</i> -OMe	4-O-	H/H	H	6.57	—	-	15	—	5
176	Me/Me	H	H	4-O-	H/H	Et	6.54	5.71	6.8	25	—	10
177	Me/MeOPr	H	H	4-O-	H/H	Et	6.43	5.73	5	22	—	5
178	Me/Me	H	<i>m</i> -OMe	4-O-	H/H	Et	5.82	5.43	2.5	8	—	18
179	Me/Me	H	<i>o</i> -OMe	4-O-	H/H	H	5.81	—	—	3	—	1
180	Me/Me	H	<i>o</i> -OMe	4-O-	H/H	Et	5.66	—	—	10	—	11
181	<i>c</i> Pr CH ₂ / <i>c</i> Pr CH ₂	H	H	4-O-	H/H	H	—	—	—	69	27	40
182	Pr/Pr	H	H	4-O-	Et/H	H	—	—	—	55	9	21
183	Pr/Me	H	H	4-O-	Me/Me	H	—	—	—	50	8	3
184	Pr/Pr	H	H	4-O-	Ph/H	H	—	—	—	47	10	5
185	Pr/Pr	H	H	4-N(CHO)	H/H	H	—	—	—	40	9	9
186	Me/Me	H	H	4-O-	Me/H	H	—	—	—	34	5	9
187	<i>i</i> -Bu/Me	H	H	4-O-	H/H	H	—	—	—	28	—	1
188	Pr/Pr	H	H	4-O-	Me/Me	H	—	—	—	26	12	6
189	Me/Me	Br	H	4-O-	H/H	H	—	—	—	24	—	4
190	Me/Me	H	H	3-O-	H/H	H	—	—	—	23	—	15
191	CF ₃ CH ₂ /CF ₃ CH ₂	H	H	4-O-	H/H	H	—	—	—	22	16	19
192	Me/	H	H	4-O-	H/H	H	—	—	—	18	—	11
193	Me/Me	H	H	4-O-	Me/Me	H	—	—	—	14	3	2
194	MeOPr/MeOPr	H	H	4-O-	H/H	H	—	—	—	12	10	9
195	Pr/Pr	H	<i>o</i> -Cl	4-O-	H/H	H	—	—	—	10	14	6
196	Pr/Pr	H	<i>o</i> -OMe	4-O-	H/H	Et	—	—	—	1	—	10
197	Pr/Pr	H	<i>o</i> -OMe	4-O-	H/H	H	—	—	—	8	—	10

^a Binding affinity values represent the mean of at least three independent experiments with a SEM always lower than 10%. ^b The binding affinity is expressed as % of radioligand displacement at the concentrations indicated in square brackets.

Table 7. Chemical Structures and binding affinities at the *hAdoR* of 9-dAX and the Corresponding Xanthine Derivatives


compd	R ₁ /R ₃	X	Z	p <i>K</i> _i ^{a,b} <i>hA</i> _{2B}	p <i>K</i> _i ^{a,b} <i>hA</i> _{2A}	<i>K</i> _i <i>hA</i> _{2A} / <i>K</i> _i <i>hA</i> _{2B}	p <i>K</i> _i ^b <i>hA</i> ₁	p <i>K</i> _i ^b <i>hA</i> ₃
7	Pr/Pr	CH	NH-C ₆ H ₄ -4Br	8.66	7.51	14.1	—	—
	Pr/Pr	N	NH-C ₆ H ₄ -4Br	8.62 ^c	5.78 ^c	700	7.13	5.63
8	Pr/Pr	CH	NH-C ₆ H ₄ -4Cl	8.80	7.50	20	—	—
	Pr/Pr	N	NH-C ₆ H ₄ -4Cl	8.10	6.72	400	7.30	5.73
9	Pr/Pr	CH	NH-C ₆ H ₄ -4F	8.48	7.92	3.6	—	—
	Pr/Pr	N	NH-C ₆ H ₄ -4F	8.65 ^d	7.78 ^d	7.5	7.74	—
21	Pr/Pr	CH	NH-C ₆ H ₅	8.03	6.65	24	—	—
	Pr/Pr	N	NH-C ₆ H ₅	8.82 ^e	8.65 ^e	17	7.39	6.86
28	Pr/Pr	CH	NH-C ₆ H ₄ -4Me	7.85	—	—	—	—
	Pr/Pr	N	NH-C ₆ H ₄ -4Me	8.72	[6.89] ^r	—	—	—
33	Pr/Pr	CH	NH-C ₆ H ₄ -4I	7.70	6.80	10	—	—
	Pr/Pr	N	NH-C ₆ H ₄ -4I	8.67	5.23	2400	6.53	5.90
41	Pr/Pr	CH	NH-C ₆ H ₄ -4CN	7.48	6.77	5.1	—	—
	Pr/Pr	N	NH-C ₆ H ₄ -4CN	8.70	6.29	260	6.39	6.24
112	Pr/Pr	CH	NH-CH ₂ C ₆ H ₅	8.50	7.05	56	—	—
	Pr/Pr	N	NH-CH ₂ C ₆ H ₅	8.50	7.70	16	7.20	6.85
165	Pr/Pr	CH	OH	7.80	6.91	8	—	—
	Pr/Pr	N	OH	7.40 ^f	[5.65] ^f	56.2	[7.2] ^r	5.40

^a Assay performed on rat AdoR are indicated by the subscript r, close to the p*K*_i affinity values reported in square brackets. ^b Binding affinity values represent the mean of at least three independent experiments with a SEM always lower than 10%; p*K*_i *hA*_{2B} and p*K*_i *hA*_{2A} determined by us, respectively. ^c 8.09 and 6.99. ^d 8.23 and 7.03. ^e 8.04 and 6.94. ^f 7.53 and 6.07. ^r = rat.

Table 8. Chemical Structures and Binding Affinities (p*K*_i) at *hA*_{2A} and *hA*_{2B} AdoRs of Various Sets of Xanthines and 9-dAX Derivatives



Y	X=N		X=N		X=CH		X=N	
	<i>hA</i> _{2A} / <i>hA</i> _{2B} ^{a)}	<i>hA</i> _{2A} / <i>hA</i> _{2B} ^{a)}	<i>hA</i> _{2A} / <i>hA</i> _{2B} ^{a)}	<i>hA</i> _{2A} / <i>hA</i> _{2B} ^{a)}	<i>hA</i> _{2A} / <i>hA</i> _{2B} ^{a)}	<i>hA</i> _{2A} / <i>hA</i> _{2B} ^{a)}	<i>hA</i> _{2A} / <i>hA</i> _{2B} ^{a)}	
4-F	<6.00/ 7.90	<6.00/ 6.73	—	—	9	7.92/ 8.48	7.78/ 8.65	
4-Br	<6.00/ 7.60	<6.00/ 7.03	—	—	7	7.51/ 8.66	5.78/ 8.62	
4-CH ₃	<6.00/ 7.72	—	—	—	28	-/ 7.85	6.89/8.72	
4-Ac	<6.00/ 7.06	—	—	—	34	-/ 7.70	—	
4-COOEt	<6.00/ 7.49	—	—	—	47	7.00/ 7.25	—	
4-I	—	—	<6.00/<6.00	<6.00/ 7.96	33	6.80/ 7.70	5.23/8.67	

^a Binding affinity values represent the mean of at least three independent experiments; the SEM (standard mean error) was always lower than 10%.

Comparable affinities at *hA*_{2B} were obtained for most of the examined 9-dAXs and 1-methyl pyrazolyl derivatives with the noticeable exception of the 4-F and 4-Br phenyl derivatives which were significantly more active in the 9-dAX series. The lack of p*K*_i data at *hA*_{2A} in Baraldi's paper¹¹ did not allow a precise comparison with 9-dAXs at this AdoR subtype. However, 9-dAXs seem to have higher *hA*_{2A} affinities than xanthines. On the whole, the above observations might suggest slightly different binding modes for xanthines and 9-dAXs at *hA*₂ receptor subtypes.

Antagonist Activity and Efficacy of Selected 9-dAX AdoR Ligands at *hA*_{2A} and *hA*_{2B} AdoR Subtypes. A number of ligands (**67–69**, **71**, **75**, and **88**, Table 9) were selected to measure their antagonistic activity and efficacy in the adenylyl cyclase functional assay at cloned *hA*_{2B} and *hA*_{2A} AdoR subtypes. A representative example of this experiment was shown in the plot of Figure 2.

The p*A*₂ values at both receptor subtypes are reported in Table 9 along with the corresponding p*K*_i values from binding assays. p*A*₂ values very close to the corresponding p*K*_is were obtained.

Table 9. Binding affinities, antagonist potency and efficacy at A_{2B} and A_{2A} receptors of selected 9-dAXs (**67–69**, **71**, **75**, and **88**)

compd	pK _i ^a hA _{2B}	pK _i ^a hA _{2A}	pA ₂ ^a hA _{2B}	pA ₂ ^a hA _{2A}	pA ₂ ^a A _{2B} ^b	pA ₂ ^a A _{2A} ^c
67	8.58	5.91	8.06	5.99	8.53	6.90
68	8.52	7.19	8.40	7.24	8.25	7.29
69	8.46	5.31	8.30	5.90	8.26	6.03
71	8.42	7.34	8.17	7.30	8.10	7.36
75	7.96	6.11	8.00	6.20	7.28	6.20
88	8.28	5.58	8.20	5.50	8.09	6.33

^a pK_i or pA₂ values represent the mean of at least three independent experiments with a SEM always lower than 10%. ^b Smooth muscle of guinea pig thoracic aorta. ^c Smooth muscle of male Sprague–Dawley rat aorta.

At hA_{2B} AdoR, the observed pK_is were always slightly higher than the corresponding pA₂ values, whereas pK_i and pA₂ values at the hA_{2A} AdoR subtype varied in a less regular way.

The antagonistic activity and efficacy of the same set of ligands were measured through functional isolated organ assay at both guinea pig A_{2B} and rat A_{2A} AdoR subtypes (see Table 9). A representative example of this assay was shown in a graphical form in Figure 3.

Again, pA₂ values very close to the corresponding pK_is were obtained. At guinea pig A_{2B} AdoR, the pA₂ values were always slightly lower than the corresponding pK_i values, whereas opposite results came from rat A_{2A} AdoR subtypes.

Conclusions

The syntheses and the analyses of the biological activity at the AdoR subtypes of a large array of 9-dAX derivatives allowed us to identify the main structural features for both high hA_{2B} affinity and hA_{2B}/hA_{2A} selectivity. A high number of 9-dAX derivatives with outstanding hA_{2B} affinity (pK_i > 8) were obtained whereas relatively few ligands with K_i hA_{2A}/K_i hA_{2B} ratio > 100 were found. Among them, results for compounds **67**, **69**, and **88** were particularly interesting both in terms of hA_{2B} affinity (pK_i = 8.58, 8.46, and 8.28, respectively) and selectivity over hA_{2A} (741, 1412, and 501, respectively). Moreover they were endowed with high selectivity also over hA₃ (> 1000, 3090, and 2344, respectively) but, regrettably, their selectivity over the hA₁ AdoR subtype was quite low (11.7, 9.3, and 3.4, respectively). This was an important unmet goal of the present study.

A number of selected ligands, tested in functional assays *in vitro*, showed very interesting antagonist activities and efficacies at both hA_{2A} and hA_{2B} AdoR subtypes, in good agreement with their affinities measured in the binding assays. We are presently working to overcome the problem of the relatively low selectivity over the hA₁ AdoR subtype, taking into account all the structural insights gained in the present and other SAR and SSR studies of AdoR ligands.

In summary, our results showed that suitably substituted 9-dAXs may represent promising highly active and hA_{2B} selective antagonists, potentially useful as antiasthmatic agents.

Experimental Section

Chemicals and solvents were from Sigma-Aldrich. When necessary, solvents were dried by standard techniques and distilled. After extraction from aqueous phases, the organic solvents were dried over anhydrous magnesium or sodium sulfate. Thin-layer chromatography (TLC) was performed by using aluminum sheets precoated with silica gel 60 F₂₅₄ (0.2 mm) type E. Merck. Chromatographic spots were visualized by UV light or Hanessian reagent.⁵³ Purification of crude compounds was carried out by flash column chromatography on silica gel 60 (Kieselgel 0.040–0.063 mm, E. Merck) or by crystallization. Melting points (uncorrected) for fully purified products (see below) were determined in a glass capillary tube on a Stuart Scientific electro thermal apparatus SMP3. ¹H NMR spectra were recorded on a 300 MHz Bruker AMX-300 spectrom-

eter. All the detected signals were in accordance with the proposed structures. Chemical shifts (δ scale) are reported in parts per million (ppm) relative to the central peak of the solvent. Coupling constant (*J* values) are given in hertz (Hz). Spin multiplicities are given as s (singlet), d (doublet), dd (double doublet), t (triplet), or m (multiplet), bs (broad singlet), dt (double triplet). Electron impact mass (EI-MS) or electron spray ionization mass (ESI-MS) were recorded in a quadrupolar Hewlett-Packard 5988 and in Waters ZQ 4000 apparatus, respectively. Elemental analyses were performed on a Carlo Erba C, H, N analyzer. Fully purified products had satisfactory (within ±0.4% of theoretical values) C, H, N analyses.

Nonhigh-throughput chemical reactions were generally carried out under an argon atmosphere whereas dry nitrogen was used in parallel syntheses. Parallel reactions were performed using a Chemspeed ASW 1000 instrument. In several instances, the final products obtained by parallel synthesis were rapidly purified by flash column chromatography up to an acceptable purity (better than 90%, HPLC check) and tested without further purification. In such a case only ESI/MS or EI/MS spectra and HPLC retention times were listed (see Table 14, Supporting Information). Mp, ¹H NMR, ESI/MS, or EI/MS spectra (Table 14, Supporting Information), and elemental analysis (Table 15, Supporting Information) were reported only for compounds prepared by traditional solution-phase synthesis (**7**, **10**, **21**, **62–65**, **67**, **68**, **70**, **71**, **74**, **75**, **80**, **83**, **85**, **96**, **99**, **112**, **133**, **135**, **137–139**, **141**, **146**, **148**, **155**, **156**, **159**, **160**, **162**, **163–171**, **173–184**, **186–197**).

The HPLC analyses were performed on a Symmetry C18 (2.1 × 10 mm, 3.5 μM) column with a Waters 2690 instrument. As detectors, Micromass ZMD for ES ionization and Waters 996 Diode Array were used. Diode array chromatograms were processed at 210 nm. The mobile phases were a mixture of formic acid (0.46 mL), aqueous ammonia 33% (0.115 mL), and water (1000 mL) (phase A) and a quaternary mixture of formic acid (0.4 mL), ammonia (0.1 mL), methanol (500 mL), and acetonitrile (500 mL) (phase B). A gradient technique was applied going from A 100% to 95% B in 20 min. The flow rate was 0.4 mL/min. The injection volume was 5 μL.

The syntheses of 1,3 dimethyl- (or -dipropyl)-6-methyl-5-nitrouracil have been already described.³³ Nonsymmetrically substituted 1,3-dialkyl-6-methyluracils were prepared by alkylation at position 3 (or 1) of the corresponding 1(3)-alkyl-6-methyluracils⁵⁴ or of the commercial 3-isobutyl-6-methyluracil.

Representative Procedure for the Condensation Reaction between Benzaldehydes and 5-Nitro-6-methyluracils to afford 1,3-Dialkyl-6-styryluracil Derivatives IV (see Scheme 1). A solution of the suitable 1,3-dialkyl-6-methyl-5-nitropyrimidine-2,4-(1*H*,3*H*)-dione **II** (30 mmol), the appropriate benzaldehyde (30 mmol), and piperidine (4.45 mL, 45 mmol) in dry dioxane (150 mL) was refluxed for 5–70 h, under argon atmosphere. The resulting solution was concentrated under vacuum, and the residue was treated with ethanol until the formation of a precipitate occurred. The solid was collected by filtration, dried under vacuum, and purified by flash column chromatography to yield the expected nitrostyryl derivatives **IV** in a sufficient purity (>95%) for the subsequent syntheses.

Representative Procedures for the Ring Closure of 5-Nitro-6-styryluracil IV to 9-dAXs V (see Scheme 1). **Method A.** A solution of the 5-nitro-6-styryluracil derivative **IV** (3.00 mmol) in triethyl phosphite (5 mL) was refluxed for 7 h. The resulting mixture

was cooled and the precipitate collected by filtration and washed with ethyl ether to yield the corresponding 1*H*-pyrrolo[3,2-*d*]-pyrimidine-2,4(3*H*,5*H*)-dione derivatives **V**, that were purified by flash column chromatography in the case of unacceptable purities.

Method B. To a solution of the appropriate 5-nitro-6-styryluracil carboxylic acid or ester **IV** (1.94 mmol) in formic acid (18 mL) was slowly added sodium dithionite (1.56 g, 9.70 mmol), and the mixture was refluxed overnight. The resulting suspension was cooled to room temperature and poured into water. The precipitate was collected by filtration, washed with water and ethyl ether, and then dried under vacuum to yield the expected 1*H*-pyrrolo[3,2-*d*]-pyrimidine-2,4(3*H*,5*H*)-dione derivatives **V**, that were purified by column chromatography, or by crystallization (water/MeOH) when necessary.

Representative Procedures for the Amidation of Oxycetic Acid and Oxycetic Ester of 9-Deazaxanthine Derivatives (V and VI, see Scheme 2). The synthesis of the target amides was performed by using one of the following methods (A–D).

Method A. The reaction took place in a sealed tube under argon atmosphere. To 0.15 mmol of the ester **V** or **VI** (see Scheme 2) and 16.00 mmol of amines was added a catalytic amount of sodium cyanide (5 mg). In the case of liquid amines the reaction mixture was heated at the boiling temperature of the amine whereas for solid amines 2 mL of anhydrous dioxane was used as solvent and the reaction heated at 100 °C. The reactions were monitored by TLC, and when no more starting material was observed, the mixture was cooled to room temperature and the final product isolated by filtration and washed with ethyl ether and recrystallized from H₂O/MeOH. When no precipitate was formed, the reaction mixture was concentrated under reduced pressure and the residue purified by flash column chromatography on silica gel.

Method B. A solution of the proper carboxylic acid (**V** or **VI**, see Scheme 2) (0.72 mmol) in anhydrous tetrahydrofuran (20 mL) under argon atmosphere was cooled to –40 °C, and *N*-methylmorpholine (0.08 mL, 0.72 mmol) and isobutyl chloroformate (0.09 mL, 0.72 mmol) were slowly added. The mixture was stirred at –40 °C for 2 h. Then the appropriate amine (0.72 mmol) was added, and the mixture was stirred 15 min at –40 °C and then for additional 12 h at room temperature. The solution was evaporated under reduced pressure, and the residue was dissolved in DCM, washed with a saturated solution of sodium bicarbonate, water, and brine, and then dried (Na₂SO₄) and evaporated under reduced pressure. The resulting crude product was purified by flash column chromatography on silica gel or crystallized by H₂O/MeOH.

Method C. To a mixture of the carboxylic acid (**V** or **VI**, see Scheme 2) (1.24 mmol), *N*-(3-dimethylaminopropyl)-*N'*-ethylcarbodiimide hydrochloride (0.28 g, 1.49 mmol), 1-hydroxybenzotriazole (0.20 g, 1.49 mmol), triethylamine (0.35 mL, 2.48 mmol), and anhydrous DCM (20 mL) was added the appropriate amine (1.61 mmol) and the mixture was stirred at room temperature overnight under argon atmosphere. The resulting solution was evaporated under reduced pressure, and the residue was dissolved in DCM and washed with a saturated sodium bicarbonate aqueous solution. The organic phase was separated, washed with water and brine, dried (Na₂SO₄), and evaporated under reduced pressure. The resulting crude was purified by flash column chromatography on silica gel or crystallized by H₂O/MeOH.

Method D. To a mixture of the carboxylic acid (**V** or **VI**, see Scheme 2) (0.21 mmol), *N*-(3-dimethylaminopropyl)-*N'*-ethylcarbodiimide hydrochloride (0.09 g, 0.23 mmol), 1-hydroxybenzotriazole (0.30 g, 0.23 mmol), and polymer-bound morpholine (0.28 g, 2.75 mmol/g based on nitrogen analysis) in anhydrous DMF (4 mL) was added the suitable amine (0.23 mmol), and the mixture was stirred overnight at room temperature. To the resulting solution were added macroporous triethylammonium methylpolystyrene carbonate (0.25 g, 2.8–3.5 mmol/g based on nitrogen elemental analysis) and Amberlyst 15 (0.65 g) as scavengers, and the suspension was stirred for 2 h (in the case of acidic or basic final products the corresponding scavenger was not added). The resulting suspension was filtered and evaporated under reduced pressure. The residue was triturated with a mixture of MeOH/ethyl ether, and

the precipitate was collected by filtration to yield the desired product in a sufficient purity for biological testing.

Biochemistry and Pharmacology. Radioligand Binding Assays. Radioligand binding competition assays were performed in vitro using A₁, A_{2A}, A_{2B}, and A₃ human receptors expressed in transfected CHO (*hA*₁), HeLa (*hA*_{2A} and *hA*₃), and HEK-293 (*hA*_{2B}) cells as described in detail in Supporting Information.

cAMP Assays. These assays were performed on *hA*_{2A} and *hA*_{2B} receptors transfected in CHO cells by using the method described by Salomon⁵⁵ as described in Supporting Information.

Isolated Organ Assays. A_{2A} Receptors. These assays were performed on *hA*_{2A} receptors⁵⁶ from isolated aorta of 200–250 g male Sprague–Dawley rats as reported in detail in Supporting Information.

A_{2B} Receptors. These assays were performed in A_{2B} receptors⁵⁷ from isolated aorta of 300–350 g male guinea pigs as reported in detail in Supporting Information.

Acknowledgment. The Italian authors thank the MIUR (Ministero dell'Istruzione, dell'Università e della Ricerca Scientifica, Rome (Italy), for partial financial support.

Supporting Information Available: Chemical, biological, and pharmacological experimental data. This material is available free of charge via the Internet at <http://pubs.acs.org>.

References

- (1) Cohn, L.; Elias, J. A.; Chupp, G. L. Asthma: mechanisms of disease persistence and progression. *Annu. Rev. Immunol.* **2004**, *22*, 789–815.
- (2) Frieri, M. Asthma concepts in the new millennium: update in asthma pathophysiology. *Allergy Asthma Proc.* **2005**, *26*, 83–8.
- (3) Szeleny, I.; Pahal, A. Drug Therapy in asthma bronchiale in the new millennium. *Pharmazie* **2002**, *57*, 83–86.
- (4) (a) Drazen, J. M.; Israel, E.; O'Byrne, P. M. Treatment of asthma with drugs modifying the leukotriene pathway. *N. Engl. J. Med.* **1999**, *340*, 197–206. (b) Kemp, J. P. Recent advances in the management of asthma using leukotriene modifiers. *Am. J. Respir. Med.* **2003**, *2*, 139–156. (c) Holgate, S. T.; Peters-Golden M. Introduction: the antiinflammatory role of cysteinyl leukotriene receptor antagonists in asthma. *Allergy Clin. Immunol.* **2003**, *111*, S1–4.
- (5) (a) Stokes, J.; Casale, T. B. Rationale for new treatments aimed at IgE immunomodulation. *Ann. Allergy Asthma Immunol.* **2004**, *93*, 212–217. (b) Babu, K. S.; Holgate S. T. The role of anti-IgE therapies in the treatment of asthma. *Hosp. Med.* **2002**, *63*, 483–6.
- (6) Marx, D.; Ezeamuzie, C. I.; Nieber, K.; Szelenyi, I. Therapy of bronchial asthma with adenosine receptor agonists or antagonists. *Drug News Perspect.* **2001**, *14*, 89–100.
- (7) Holgate, S. T. The identification of the adenosine A_{2B} receptor as a novel therapeutic target in asthma. *Br. J. Pharmacol.* **2005**, *145*, 1009–1015.
- (8) Jacobson, K. A.; IJzerman, Ad P.; Linden, J. 1,3-Dialkylxanthine derivatives having high potency as Antagonist at human A_{2B} adenosine receptor. *Drug. Dev. Res.* **1999**, *47*, 45–53.
- (9) Klingler, M.; Freissmuth, M.; Nanoff, C. Adenosine receptors: G protein-mediated signalling and the role of accessory proteins. *Cell Signal.* **2002**, *14*, 99–108.
- (10) Fredholm, B. B.; IJzerman, A. P.; Jacobson, K. A.; Klotz, K. N.; Linden, J. International Union of Pharmacology. XXV. Nomenclature and classification of adenosine receptors. *Pharmacol. Rev.* **2001**, *53*, 527–552.
- (11) Baraldi, P. G.; Tabrizi, M. A.; Preti, D.; Bovero, A.; Romagnoli, R.; Fruttarolo, F.; Zaid, N. A.; Moorman, A. R.; Varani, K.; Gessi, S.; Merighi, S.; Borea, P. A. Design, synthesis, and biological evaluation of new 8-heterocyclic xanthine derivatives as highly potent and selective human A_{2B} adenosine receptor antagonists. *J. Med. Chem.* **2004**, *47*, 1434–1447.
- (12) Volpini, R.; Costanzi, S.; Vittori, S.; Cristalli, G.; Klotz, K. N. Medicinal chemistry and pharmacology of A_{2B} adenosine receptors. *Curr. Top. Med. Chem.* **2003**, *3*, 427–443.
- (13) Cristalli, G.; Lambertucci, C.; Taffi, S.; Vittori, S.; Volpini, R. Medicinal chemistry of adenosine A_{2A} receptor agonists. *Curr. Top. Med. Chem.* **2003**, *3*, 387–401.
- (14) Müller, C. E.; Stein, B.; Adenosine receptor antagonists: structure and potential therapeutic applications. *Curr. Pharm. Des.* **1996**, *2*, 501–530.
- (15) Baraldi, P. G.; Borea, P. A. New potent and selective human adenosine A₃ receptor antagonists. *Trends Pharmacol. Sci.* **2000**, *21*, 456–459.

- (16) Baraldi, P. G.; Cacciari, B.; Romagnoli, R.; Merighi, S.; Varani, K.; Borea, P. A.; Spalluto, G. A3 adenosine receptor ligands: history and perspectives. *Med. Res. Rev.* **2000**, *20*, 103–128.
- (17) van der Wenden, E. M.; IJzerman, A. P.; Soudijn, W. A. Steric and electrostatic comparison of three models for the agonist/antagonist binding site on the adenosine A1 receptor. *J. Med. Chem.* **1992**, *35*, 629–635.
- (18) Kim, Y. C.; Ji, X.; Melman, N.; Linden, J.; Jacobson, K. A. Anilide derivatives of an 8-phenylxanthine carboxylic congener are highly potent and selective antagonists at human A2B adenosine receptors. *J. Med. Chem.* **2000**, *43*, 1165–1172.
- (19) Baraldi, P. G.; Cacciari, B.; Moro, S.; Spalluto, G.; Pastorin, G.; Da Ros, T.; Klotz, K.-N.; Varani, K.; Gessi, S.; Borea, P. A. Synthesis, biological activity, and molecular modeling investigation of new pyrazolo[4,3-*e*]-1,2,4-triazolo[1,5-*e*]pyrimidine derivatives as human A3 adenosine receptor antagonists. *J. Med. Chem.* **2002**, *45*, 770–780.
- (20) Soudijn, W.; van, Weden., I.; IJzerman, A. P. Medicinal chemistry of adenosine A1 receptor ligands. *Curr. Top. Med. Chem.* **2003**, *3*, 355–367.
- (21) Müller, C. E. Medicinal chemistry of adenosine A3 receptor ligands. *Curr. Top. Med. Chem.* **2003**, *3*, 445–462.
- (22) DeNinno, M. P.; Masamune, H.; Chenard, L. K.; DiRico, K. J.; Eller, C.; Etienne, J. B.; Tickner, J. E.; Kennedy, S. P.; Knight, D. R.; Kong, J.; Oleynek, J. J.; Tracey, W. R.; Hill, R. J. 3'-Aminoadenosine-5'-uronamides: discovery of the first highly selective agonist at the human adenosine A3 receptor. *J. Med. Chem.* **2003**, *46*, 353–355.
- (23) Kim, Y. C.; Ji, X.; Melman, N.; Linden, J.; Jacobson, K. A. Anilide derivatives of an 8-phenylxanthine carboxylic congener are highly potent and selective antagonists at human A2B adenosine receptors. *J. Med. Chem.* **2000**, *43*, 1165–1172.
- (24) Hayallah, A. M.; Sandoval-Ramirez, J.; Reith, U.; Schobert, U.; Preiss, B.; Schumacher, B.; Daly, J. W.; Müller, C. E. 1,8-disubstituted xanthine derivatives: synthesis of potent A2B-selective adenosine receptor antagonists. *J. Med. Chem.* **2002**, *45*, 1500–1510.
- (25) Kim, S. A.; Marshall, M. A.; Melman, N.; Kim, H. S.; Müller, C. E.; Linden, J.; Jacobson, K. A. Structure–activity relationships at human and rat A2B adenosine receptors of xanthine derivatives substituted at the 1-, 3-, 7-, and 8-positions. *J. Med. Chem.* **2002**, *45*, 2131–2138.
- (26) Baraldi, P. G.; Tabrizi, M. A.; Preti, D.; Bovero, A.; Fruttarolo, F.; Romagnoli, R.; Moorman, A. R.; Gessi, S.; Merighi, S.; Varani, K.; Borea, P. A. [3H]-MRE 2029-F20, a selective antagonist radioligand for the human A2B adenosine receptors. *Bioorg. Med. Chem. Lett.* **2004**, *14*, 3607–3610.
- (27) Hansel, T. T.; Tennant, R. C.; Tan, A. J.; Higgins, L. A.; Neighbour, H.; Erin, E. M.; Barnes, P. J. Theophylline: mechanism of action and use in asthma and chronic obstructive pulmonary disease. *Drugs Today (Barc.)* **2004**, *40*, 55–69.
- (28) Maconi, A.; Pastorin, G.; Da Ros, T.; Spalluto, G.; Gao, Z. G.; Jacobson, K. A.; Baraldi, P. G.; Cacciari, B.; Varani, K.; Moro, S.; Borea, P. A. Synthesis, biological properties, and molecular modeling investigation of the first potent, selective, and water-soluble human A3 adenosine receptor antagonist. *J. Med. Chem.* **2002**, *45*, 3579–3582.
- (29) Ongini, E.; Monopoli, A.; Cacciari, B.; Baraldi, P. G. Selective adenosine A2A receptor antagonists. *Farmacologia* **2001**, *56*, 87–90.
- (30) Müller, C. E. A1 adenosine receptors and their ligands: overview and recent developments. *Farmacologia* **2001**, *56*, 77–80.
- (31) Hayallah, A. M.; Sandoval-Ramirez, J.; Reith, U.; Schobert, U.; Preiss, B.; Schumacher, B.; Daly, J. W.; Müller, C. E. 1,8-Disubstituted xanthine derivatives: synthesis of potent A2B-selective adenosine receptor antagonists. *J. Med. Chem.* **2002**, *45*, 1500–1510.
- (32) Baraldi, P. G.; Romagnoli, R.; Tabrizi, M. A.; Bovero, A.; Preti, D.; Fruttarolo, F.; Moorman, A. R.; Borea, P. A. New heterocyclic ligands for the adenosine receptors P1 and for the ATP receptors P2. *Farmacologia* **2005**, *60*, 185–202.
- (33) Grahner, B.; Winiwarter, S.; Lanzner, W.; Müller, C. E. Synthesis and structure–activity relationships of deazaxanthines: analogues of potent A1- and A2-adenosine receptor antagonists. *J. Med. Chem.* **1994**, *37*, 1526–1534.
- (34) Stefanachi, A.; Leonetti, F.; Cappa, A.; Carotti, A. Fast and highly efficient one-pot synthesis of 9-deazaxanthines. *Tetrahedron Lett.* **2003**, *44*, 2121–2123.
- (35) Carotti, A.; Stefanachi, A.; Raviña, E.; Sotelo, E.; Loza, M. I.; Cadavid, M. I.; Centeno, N. B.; Nicolotti, O. 8-Substituted-9-deazaxanthines as adenosine receptor ligands: design, synthesis and structure-affinity relationships at A2B. *Eur. J. Med. Chem.* **2004**, *39*, 879–887.
- (36) Vidal, B. J.; Esteve Trias C.; Segarra Matamoros, V.; Ravina Rubira, E.; Fernandez Gonzales, F.; Loza Garcia, M. I.; Sanz Carreras, F. 6-Phenyldihydropyrrrolo pyrimidinedione, 2003, WO 033694.
- (37) Senda, S.; Suzui, A.; Honda, M.; Fujimura, H. Uracil derivatives and related compounds. III. 5-Amino-1,3,6-trialkyluracil derivatives. *Chem. Pharm. Bull.* **1958**, *6*, 482–487.
- (38) Papesch, V.; Dodson, R. M. G. D. Pyrimido[5,4-*d*][1,2,3]triazines. *J. Org. Chem.* **1963**, *28*, 1329.
- (39) Bicking, J. B.; Robb, C. M.; Watson, L. S.; Cragoe, E. J., Jr. (Vinylaryloxy)acetic acids. A new class of diuretic agents. 2. (4-(3-Oxo-1-alkenyl)phenoxy)acetic acids. *J. Med. Chem.* **1976**, *19*, 544–547.
- (40) Agarwal, R.; Chaudray, C.; Singh, C. J.; Misra, V. S. Synthesis of 2-methoxy-4-(3-methyl-5-oxo-1-phenyl-4-pyrazolyldenemethyl)phenoxyacetic acid and its ethyl ester. *Indian J. Med Chem Sect. B Org. Chem. Includ. Med Chem* **1982**, *21B*, 152–153.
- (41) Albericio, F.; Barany, G. An acid-labile anchoring linkage for solid-phase synthesis of C-terminal peptide amides under mild conditions. *Int. J. Pept. Protein Res.* **1987**, *30*, 206–216.
- (42) Tipson, R. S. Antiviral Activity of 2,2-dichloro-4'-formylacetoanilide thiosemicarbazone. *J. Med. Chem.* **1963**, *35*, 216–217.
- (43) Cheng, M. F.; Fang, J. M. Liquid-phase combinatorial synthesis of 1,4-benzodiazepine-2,5-diones as the candidates of endothelin receptor antagonism. *J. Comb. Chem.* **2004**, *6*, 99–104.
- (44) Behrens, G.; Hildenbrand, K.; Schulte-Frohlinde, D.; Herak, J. N. Reaction of sulfate radical anion with methylated uracils. An electron spin resonance study in aqueous solution. *J. Chem. Soc., Perkin Trans. 2* **1988**, *3*, 305–307.
- (45) Aichner, J.; Egg, H.; Gapp, D.; Haller, S.; Rakowitz, D.; Ramspacher, U. Insight into novel cyclization reactions using acetic anhydride in the presence of 4-dimethylaminopyridine. *Heterocycles* **1993**, *36*, 307–311.
- (46) Senda, S.; Suzui, A. Uracil derivatives and related compounds. I. Condensation of monosubstituted urea and ethyl acetoacetate. *Chem. Pharm. Bull.* **1958**, *6*, 476–479.
- (47) Boese, A. B. 4-methyluracil and its homologs, US patent, 1938, 2,138,758.
- (48) Senda, S.; Hirota, K.; Banno, K. Pyrimidine derivatives and related compounds. 15. Synthesis and analgetic and antiinflammatory activities of 1,3-substituted 5-amino-6-methyluracil derivatives. *J. Med. Chem.* **1972**, *15*, 471–476.
- (49) Tipson, R. S. Antiviral Activity of 2,2-dichloro-4'-formylacetoanilide thiosemicarbazone. *J. Med. Chem.* **1963**, *35*, 216–217.
- (50) Tani, M.; Ikegami, H.; Tashiro, M.; Hiura, T.; TsuiKioaka, H.; Kaneko, C.; Notoya, T.; Shimizu, M.; Uchida, M.; Regioselective Bromination of methoxy derivatives of ethyl indole-2-carboxylate [Synthetic studies of indoles and related compounds]. *Heterocycles* **1992**, *34*, 2349–2362.
- (51) Högberg, T.; Ström, P.; Ebner, M.; Råmsby, S. Cyanide as an efficient and mild catalyst in the aminolysis of esters. *J. Org. Chem.* **1987**, *52*, 2033–2036.
- (52) Jacobson, K. A.; Ukena, D.; Padgett, W.; Daly, J. W.; Kirk, K. L. Xanthine functionalized congeners as potent ligands at A2-adenosine receptors. *J. Med. Chem.* **1987**, *30*, 211–214.
- (53) Touchstone, J. *Advances in Thin-Layer Chromatography*; Wiley: New York, 1982.
- (54) Nieto, R. M.; Coelho, A.; Martinez, A.; Stefanachi, A.; Sotelo, E.; Ravina, E. Synthesis of 1-substituted-6-methyluracils. *Chem. Pharm. Bull.* **2003**, *51*, 1025–1028.
- (55) Salomon, Y. Adenylate cyclase assay. *Adv. Cyclic Nucleotide. Res.* **1979**, *10*, 35–55.
- (56) Prentice, D. J.; Hourani, S. M. O. Activation of multiple sites by adenosine analogues in the rat isolated aorta. *Br. J. Pharmacol.* **1996**, *118*, 1509–1517.
- (57) Alexander, S. P.; Losinsky, A.; Kendall, D. A.; Hill, S. J. A comparison of A2 adenosine receptor induced cyclic AMP generation in cerebral cortex and relaxation of pre-contracted aorta. *Br. J. Pharmacol.* **1994**, *111*, 185–190.